FORSCHUNGSZENTRUM JÜLICH GmbH

Institut für Sicherheitsforschung
und Reaktortechnik

Source Term Estimation for Small Sized HTRs

Rainer Moormann

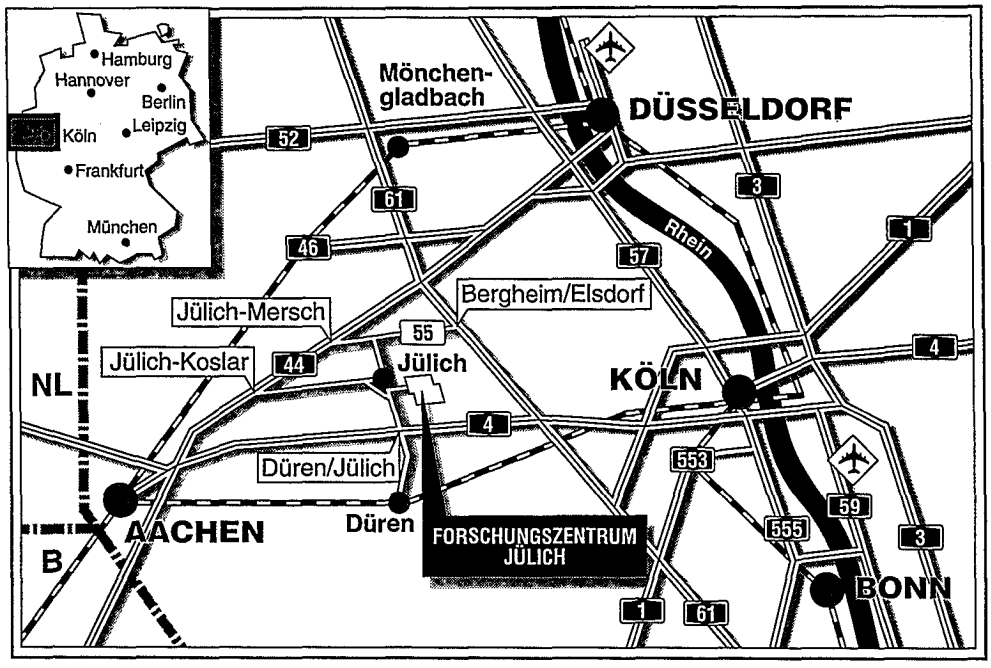

Berichte des Forschungszentrums Jülich ; 2669
ISSN 0366-0885
Institut für Sicherheitsforschung und Reaktortechnik Jül-2669

Zu beziehen durch: Forschungszentrum Jülich GmbH · Zentralbibliothek
Postfach 1913 · D-5170 Jülich · Bundesrepublik Deutschland
Telefon: 02461/61-6102 · Telefax: 02461/61-6103 · Telex: 833556-70 kfa d

Source Term Estimation for Small Sized HTRs

Rainer Moormann

ABSTRACT

A survey on methods and data relevant for source term estimations of modern small HTRs, which are equipped with a high safety standard, is given. Accidents which have to be considered are core heat-up, reactivity transients, water or air ingress and primary circuit depressurization. The main effort of this paper belongs to water/air ingress and depressurization, which requires consideration of fission product plate out under normal operation conditions; for the latter it is clearly shown, that absorption (penetration) mechanisms are much less important than assumed sometimes in the past. Source term estimation procedures for core heat-up events are shortly reviewed; reactivity transients are apparently covered by them. Besides a general literature survey including identification of areas with insufficient knowledge this paper contains some estimations on the thermochemical behaviour of fission products in water and air ingress accidents. Typical source term examples are also presented. In an appendix, evaluations of the AVR experiments VAMPYR-I and -II with respect to plate out and fission product filter efficiency are outlined and used for a validation step of the new plate out code SPATRA.

CONTENT page

1. INTRODUCTION

The philosophy of the modular German High Temperature Reactor (HTR) is based on the concept of inherent safety features, which means, that significant consequences of accidents may be excluded as far as possible without active measures (like emergency cooling, filters etc.). This concept has to be applied not only for design basis accidents but also for hypothetical events in the frequency regime usually examined in safety studies ($>10^{-7}a^{-1}$). Details to the design of the HTR-Modul are found elsewhere /6/; some general design characteristics of the modular HTR are given in fig. 1 and tab. I.

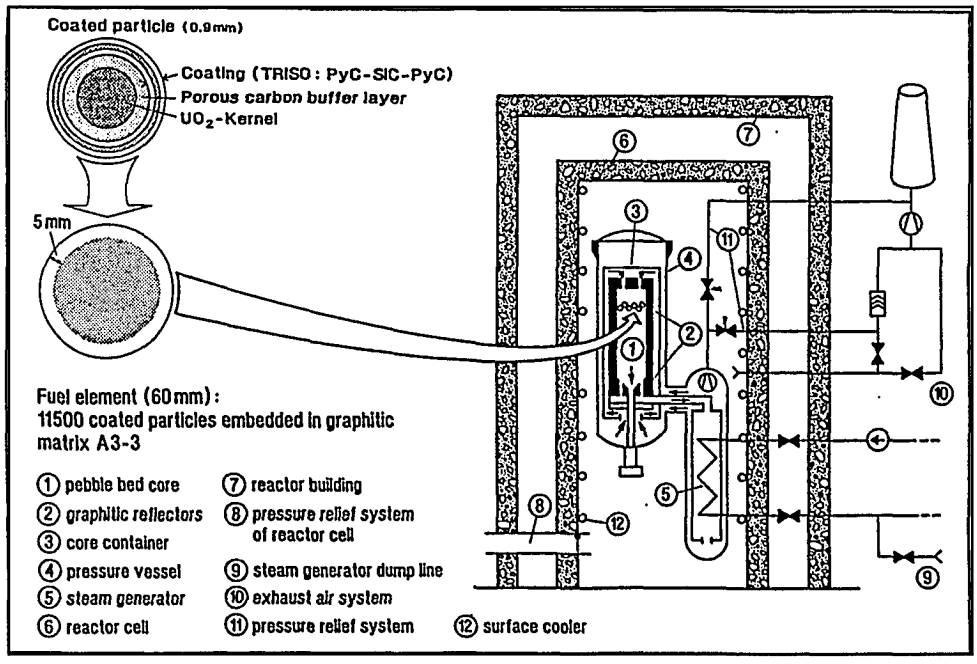

Schematic diagram of the HTR-Modul with its barriers for fission product release

Fig. 1

At the beginning of an accident, nearly all fission products are enclosed in intact coated particles. There are 3 mechanisms, leading to a massive release of this fission product inventory: Temperature increase of at least some hundred *K* beyond fuel element design values (1523 *K* = 1250°*C*) in course of core heat-up accidents, long term graphite burning with

Thermal / Electric power [MW]	200 / 80
Thermal power density [MW · m^{-3}]	3.0
Cooling medium / pressure [MPa] / flow [kg · s^{-1}]	He / 6.0 / 85
Maximum fuel temperature in normal operation [K]	1123
He inlet / outlet temperature [K]	523 / 973
Pebble bed height / diameter [m]	9.5 / 3.0
Fuel type	8 % enriched Uranium as UO_2
Uranium content in a fuel element [kg]	$7 \cdot 10^{-3}$
Maximum burn-up [% fima]	9
Operation time of a fuel element [d]	1100
Number of fuel element pebbles	$3.6 \cdot 10^5$
Emergency cooling system	—
Pressure vessel	steel vessel
Reactor building	confinement

Main design data of the HTR-Modul

Tab. I

destruction of fuel elements due to an air ingress, or heavy criticallity excursion.

As will be shown later in detail, the design of modern small HTRs excludes temperatures in core heat-up accidents, where significant release of this fission product inventory may occur. This is obtained by low power and power density of the HTR-core, by a high surface to volume ratio of the core and by a steel vessel, allowing an efficient heat-transfer to the surroundings.

Long term graphite burning is nearly excluded by the design of the pressure vessel inclusive its interior and of the reactor building, severely limiting the probability of high air ingress rates into the graphitic core. Heavy criticallity excursions are very rare events, because of the nuclear design of the HTR-Modul, in particular its low uranium/moderator ratio in the fuel. Extremly fast reactivity transients as such, which are known to destroy particle coatings /14/, are difficult to imagine in this reactor.

As will be explained in chapter 3, there is a small amount of fission products outside intact particles at accident initiation which is easier released than the intact particle inventory. Source terms of core heat-up and (limited) air ingress accidents in modular HTRs are mainly restricted to this inventory. This is also true for reactivity transients within the above outlined frequency regime, whose source term handling is covered by core heat-up events. In case of core heat-up, a small part of some metallic fission products, enclosed in intact coated particles, may also be released.

Release mechanisms in core heat-up accidents are:

Temperature induced

- diffusion in particle kernel and graphite for particles with defective coatings and, in addition, in coatings for intact particles
- coating failure
- diffusion in graphite kernels for activity, resulting from heavy metal contamination of the matrix graphite
- desorption of activity, plated out on primary circuit surfaces

A (limited) air ingress, which might be combined with a core heat-up event, may significantly increase the mobilization of fission products, beeing outside coated particles. This is due to

- oxidative gasification of graphite, combined with release of its fission product inventory

- oxidative interaction of oxygen with UO_2 in particles with defective coatings, leading to an enhanced release of iodine, noble gases and perhaps cesium
- oxygen attack on metallic primary circuit surfaces, causing a fission product desorption

Similar mechanisms as for (limited) air ingress are valid for steam ingress into the primary circuit, too. Ingressing liquid water might cause a mechanical decontamination of surfaces by erosive forces; also, the high solution capability of liquid water might contribute to an increase of activity mobilization from surfaces. Subsequent evaporation of the water transfers the fission products into the gas phase. Steam/water ingress accidents are more frequent than air ingress and, accordingly, of higher safety relevance.

A (complete or partial) depressurization of the primary circuit occurs in combination with all safety relevant sequences of the above listed accidents, because a release path into the environment is possible only in combination with an opening in the primary circuit enclosure. If depressurization occurs, before fission product mobilization into the gas phase takes place -as is usually the case for core heat-up and air ingress accidents- transport of the mobilized (gas borne) activity into the environment remains small because of a lack of an efficient transport mechanism: Under these circumstances, only thermal expansion of the primary circuit gas inventory, diffusion or atmospheric pressure variations may cause a transport. In case of depressurization following mobilization, as for relevant water ingress scenarios, this transport is much more efficient due to the depressurization itself.

However, a (partial) depressurization may also proceed as an isolated event. In any case, the following source term contributions initiated by the depressurization process have to be taken into account:

- release of the fission product inventory of the cooling gas (equilibrium concentration of the normal operating reactor, and the above outlined contributions of preceeding accident steps)
- desorption of activity, plated out on surfaces, due to the concentration drop of the fission products in the gas phase
- partial release of dust borne activity by lift-off of settled dust due to flow induced shear forces.

Considering the HTR-typical source term vector /1,2/ in combination with German regulations for design basis accidents /4/ and emergency

planning /5,71/ or with more realistic accident consequence models /3/ the following nuclides have been identified as most important for HTR safety analyses: Sr-90, I-131, Cs-134, Cs-137. For certain conditions, also other iodine isotopes, noble gases and Ag-110m have to be taken into account. In general, I-131 is most important for design and emergency planning (maximum individual doses are limiting factors), whereas Cs-137 dominates the consequences in realistic models (which are based on collective doses). However, there is a tendency to apply the more restrictive German design rules also for hypothetical events of inherent safe nuclear reactors in order to proof their safety features. One reason for doing this was, that the more realistic consequence models lead to consequences (late fatalities) in the event frequency range of $\geq 10^{-7}a^{-1}$, which are so small for the HTR-Modul, that they are not really meaningfull. Nevertheless, dose estimation by these more realistic models is reasonable also for the low source terms in the above mentioned frequency range of the HTR-MODUL. Some additional informations on dose estimations are presented in App. E.

In the following chapters, an overview on the source term estimation for these nuclides in modern small HTRs, in particular for the modular HTR, is given. At first, facts leading to the exclusion of massive releases are presented. After that, the fission product distribution at accident initiation on intact/defective coated particles, graphite contamination, plate out- and dust borne activity will be outlined, because this distribution remarkably influences the dominant source terms. At last, methods and data for source term estimation of the above listed accidents will be explained and some examples of source term estimations performed by KFA/ISF resp. ISR for the HTR-Modul will be presented; important areas of lack of knowledge will also be defined. Core heat-up events are only shortly described, because they are considered elsewhere in detail /8,11/.

2. EXCLUSION OF SEVERE FISSION PRODUCT RELEASE: STATUS AND LIMITS

In the following chapters it will be shown, that severe fission product release can be excluded until far into the hypothetical range. Nevertheless, some very hypothetical accident scenarios may lead to a large release; state of knowledge and future work in this field are explained.

2.1 Source terms in unrestricted core heat-up events and in criticality excursions

By heating of irradiated HTR fuel elements up to some weaks it was shown /7,8/, that a significant release of radiological important fission products may not happen at temperatures < 1600-1650°C = 1873-1923 K. A typical result of such heating experiments is presented in Fig. 2.

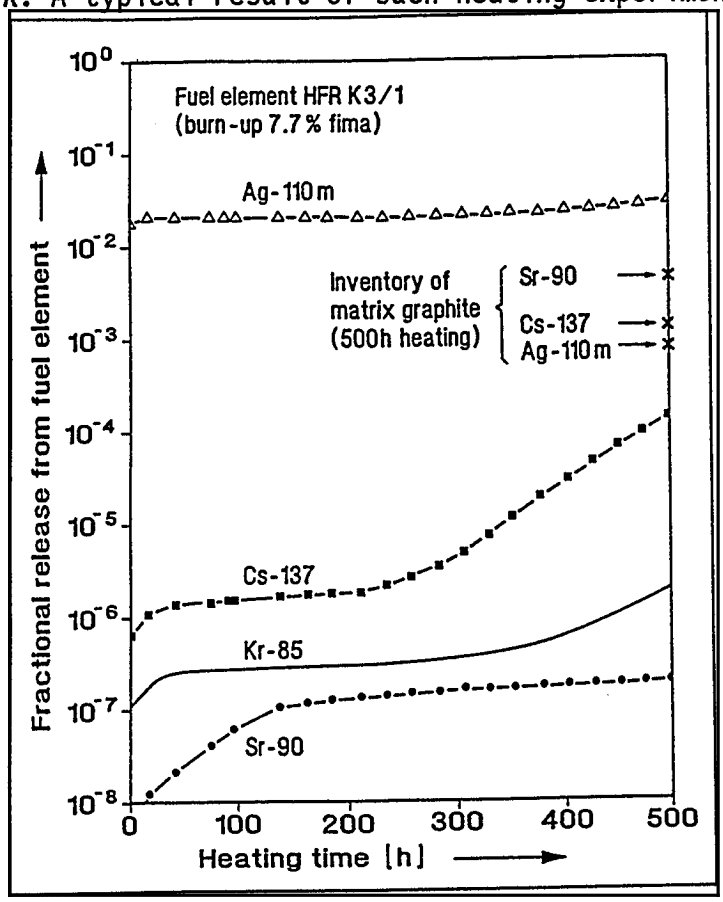

Fission product release of a long-term fuel element heating experiment at 1873 K (≙1600 °C)

Fig. 2

Release of Kr-85, which shows similar release behaviour as I-131, may be taken as indicator for defective particle coatings, because its diffusion in intact coatings is negligible but fast at 1600°C=1873 K in particle kernels and no retention occurs in graphite; the low release of Kr-85 indicates, that all coatings remain intact during heating and that no defective particles by production or irradiation exist in this particular fuel element. Whereas the high temperature stability of coatings is an outcome of all heating experiments at this temperature, about each second fuel element contains one coating defect by fabrication or irradiation, as will be shown in chapter 3.1.

Cesium and strontium diffuse slowly via intact coatings, as their inventory in graphite after 500 *h* of heating indicate. However, the strong chemisorption of these elements by the fuel element graphite prevents a significant release, in particular for strontium. Extrapolating to the whole core, this retention on graphite increases by some orders of magnitude because chemisorption of gas borne cesium and strontium takes place on colder fuel elements and on the reflectors, as will be outlined in chap. 4.1.2. Release of Ag-110m is comparably high due to its fast diffusion in fuel element components and bad retention on graphite; its amount in the fuel, however, is small (total inventory: $2 \cdot 10^5$ *GBq*).

Thermohydraulic estimations for the HTR-Modul indicate, that also for worst core heat-up conditions concerning core temperatures (fast primary circuit depressurization, no reactor cooling) the maximum fuel temperature remains below 1575°*C*= 1848 *K*; only 3 % of the fuel elements reach temperatures >1500°*C*=1773 *K* for less than 2.5 days /9/. Taking into account, that < 10^{-4} of the fission product inventory is outside intact coated particles at accident initiation (s. chapter 3.1), a significant fission product release in core heat-up events may be excluded.

The temperature behaviour in more frequent (but nevertheless hypothetical) reactivity transients is covered by the above outlined values for core heat-up events /10/. Accordingly, severe release may not occur in these accidents. However, for some highly hypothetical fast reactivity transients in combination with water ingress some irradiation experiments will be performed in the ARGUS-pulse-reactor (Moscow) on fuel elements; the irradiated fuel elements will be heated up to 1600°*C* = 1873 *K* in KFA hot cells. The data of these experiments will be used in development of a particle failure model for such reactivity accidents.

More detailed information about the source term limitation of small HTRs in core heat-up events are found elsewhere /1,2,8,11/.

2.2 Massive long term air ingress

Long term air ingress with graphite burning /12/ is possible only by natural convection (chimney draught) due to 2 leaks in top and bottom position of the pressure vessel and an additional leak in the inner core container, due to 1 big sized leak in pressure vessel and core container or (in case of the HTR-Modul) due to a complete rupture of

the coaxial duct. In addition, there must be a path between the leak(s) in the pressure vessel and the environment; that means, the reactor building may not act act as a significant barrier for gas exchange. Accident scenarios, leading to such configurations are not easily imaginable; their frequency will be $<< 10^{-7}\ a^{-1}$, i.e. in a very hypothetical regime.

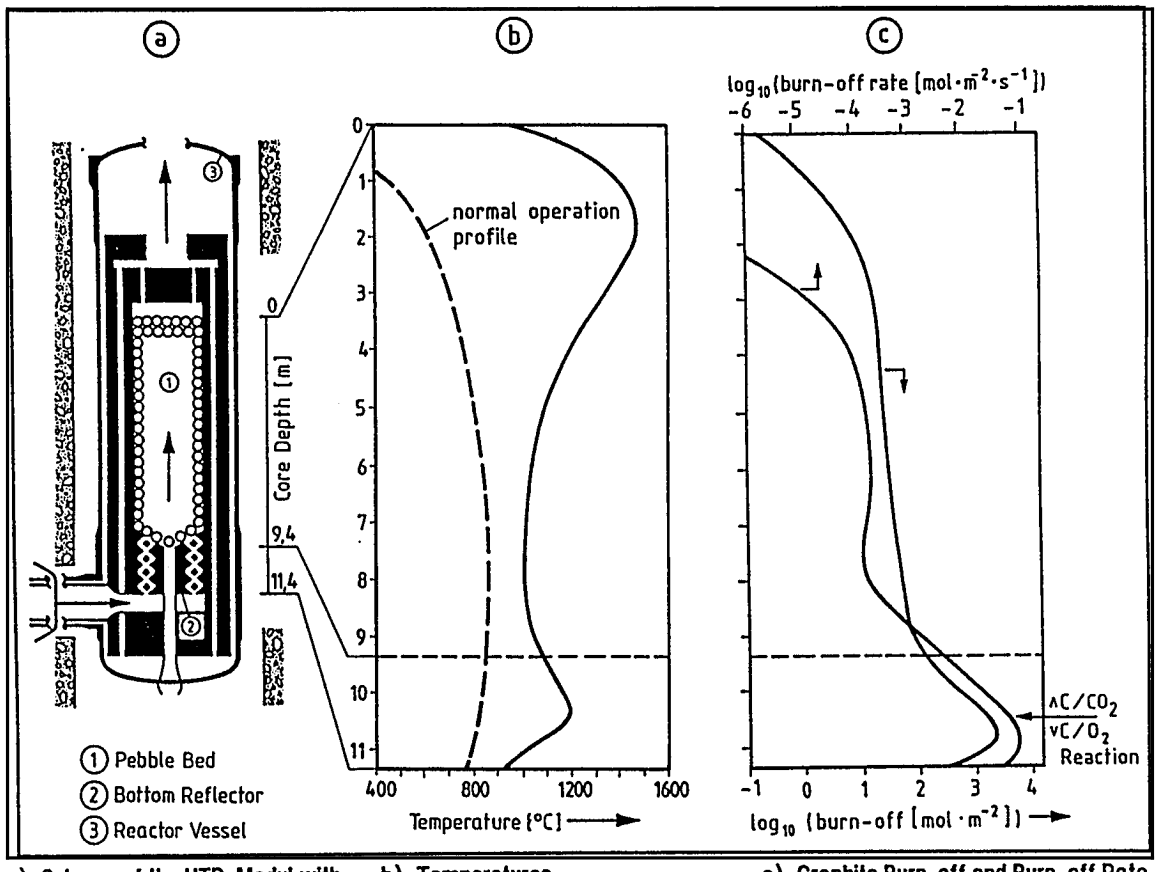

a) Scheme of the HTR-Modul with Flow Paths in the Case of a Chimney Draught Accident

b) Temperatures ... ... along the Central Axis of the Core for Massive Air Ingress Caused by a Chimney Draught (0.3 kg·s^{-1}, 20 h after air ingress initiation)

c) Graphite Burn-off and Burn-off Rate ...

Fig. 3

Nevertheless, parametric calculations have been executed for such severe air ingress conditions /12/, using the code REACT/THERMIX /13/. One example of a REACT/THERMIX-result on severe air ingress in the HTR-Modul is presented in fig. 3, indicating, that the C/O_2-reaction front remains within the bottom reflector whereas fuel element oxidation occurs via the endothermic Boudouard-reaction; this behaviour is typical for accident sequences with hot bottom reflector at accident initiation. Summing up, these calculations indicate for the (most credible) sequences with gas flow to the core via the (hot) bottom reflector a significant time span between start of air ingress and first setting free of coated particles due to graphite oxidation (which occurs in the active core mainly by the Boudouard reaction). This also holds for high

air ingress rates /12/ restricted only by the flow resistance within the pebble bed core. Setting free of coated particles does not necessarily mean coating destruction and fission product release, because the SiC-coating will be converted by oxidative attack into SiO_2. The latter seems to inhibit significantly a further progress of particle corrosion at least at temperatures well below its melting point (>1600°*C*=1873 *K*); for highly corroded regions active core temperatures calculated with REACT/THERMIX remain below 1500°*C* = 1773 *K* for at least 2 days.

As an example of the oxidation behaviour of particles fig. 4 shows REM-pictures of an oxidized (300 *h* in air, 950°*C* = 1223 *K*) and an unoxidized unirradiated coated TRISO particle.

As may be seen, the outer pyrocarbon is removed by oxidation but the SiC layer is not visibly corroded. NUKEM-experiments on TRISO-particles indicated the same: After 50 h of heating in air (1100°*C*=1373 *K*) the fraction of defect SiC layers increased only from $3.3 \cdot 10^{-5}$ to $2.5 \cdot 10^{-4}$ /72/. Some irradiated DRAGON TRISO fuel has been burned and no significant increase in the defect layer level has been detected (700-1000°*C* = 973-1273 *K*, 5 - 15 *h*) /74/; however, the original defect fraction of these particles was already high (10^{-2}). The behaviour of irradiated fuel elements in air at temperatures up to 1600°*C*=1873 *K* will be examined experimentally in future in KFA/IRW in order to validate the oxidation resistance of particles under severe air ingress conditions.

However, also with the worst case assumption, that setting free of particles is identical with total release of its fission product content, the time span between accident initiation and start of massive release seems to allow for counter measures like covering of the leaks /12/; this time span is increased, if only a complete rupture of the coaxial duct is assumed and no additional leaks are considered at the top of the pressure vessel. The comparatively easy realization of such accident management measures should be taken into consideration in general assessments of those accidents. Additional analytical and experimental work on thermohydraulics and graphite oxidation in severe air ingress by chimney draught in the HTR-Modul will be performed in the next time in KFA-ISR; research work on an outer coating of fuel elements in order to prevent burning is included.

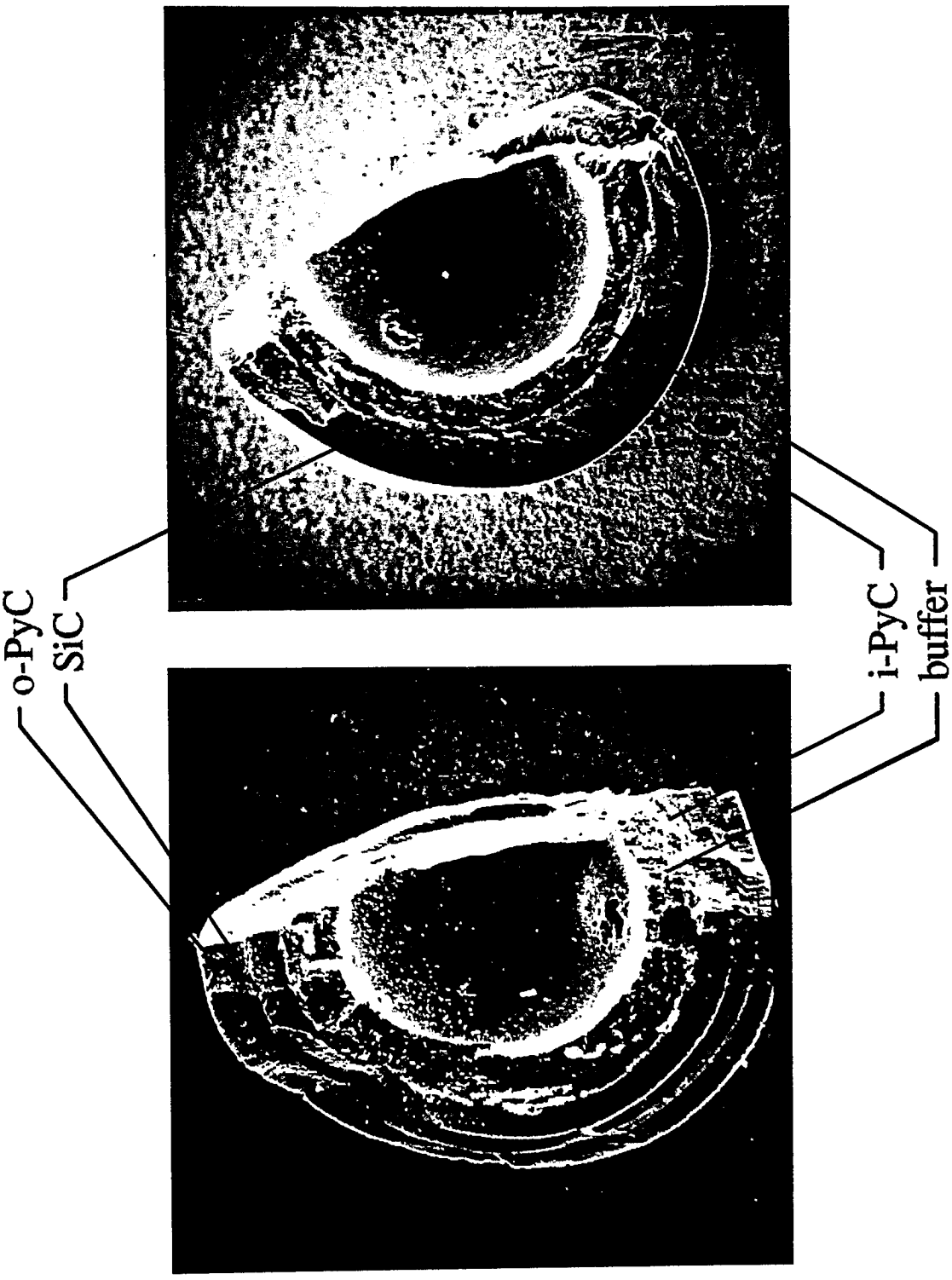

Fig. 4: REM-pictures of (broken) TRISO-coated particles: Left: uncorroded, right: corroded for 300 *h* in air at 950°*C* = 1223 *K*.

3. FISSION PRODUCT DISTRIBUTION WITHIN THE PRIMARY CIRCUIT AT ACCIDENT INITIATION

3.1 General remarks

Inventory in \ Nuclide	Cs-137	Sr-90	I-131	Xe-133
Particles with intact coatings	>0.9998	0.9999	>0.9999	>0.9999
Kernels of particles with defective coatings	$5 \cdot 10^{-5}$	$5 \cdot 10^{-5}$	$5 \cdot 10^{-5}$	$5 \cdot 10^{-5}$
Carbon buffer layer of particles with defective coatings	$1 \cdot 10^{-6}$	$1 \cdot 10^{-6}$	$1 \cdot 10^{-6}$	$1 \cdot 10^{-6}$
Grains of matrix graphite (recoil from Uranium contamination into matrix material)	$<1 \cdot 10^{-6}$	$<1 \cdot 10^{-6}$	$<1 \cdot 10^{-6}$	$<1 \cdot 10^{-6}$
Inner surfaces of matrix graphites and reflector graphites (chemisorbed during diffusion from cooling gas or coated particle into the porous graphite)	$2 \cdot 10^{-5}$	$1 \cdot 10^{-5}$	$(4 \cdot 10^{-7})$	—
Metallic primary circuit components (plate-out)	$5 \cdot 10^{-5}$	$2 \cdot 10^{-6}$	$2 \cdot 10^{-7}$	—
Settled dust a) primary circuit b) clean-up plant	a) $1 \cdot 10^{-6}$ b) $<2 \cdot 10^{-8}$	a) $4 \cdot 10^{-8}$ b) $<8 \cdot 10^{-10}$	a) $1 \cdot 10^{-8}$ b) $2 \cdot 10^{-10}$	—
Cooling gas	$<1 \cdot 10^{-11}$	$<1 \cdot 10^{-12}$	$<1 \cdot 10^{-10}$	$<6 \cdot 10^{-7}$
Overall inventory [GBq]	$1.7 \cdot 10^{7}$	$1.4 \cdot 10^{7}$	$2.1 \cdot 10^{8}$	$4.5 \cdot 10^{8}$

Fractional distribution of some fission products in the HTR-Modul following 30 a of operation (Best estimate values)

Tab. II

Table II lists the fission product inventory within the primary circuit of the HTR-Modul, following 30-years of normal operation; this inventory is divided in different groups, which have to be handled separately in source term estimations. Methods and data, used for evaluation of these values are as follows: Fission product release from core is estimated for metallic fission products with help of the diffusion model FRESCO-II /19/ and with a Booth-model for short-living nuclides (code STADIF-II /90/). Gaseous precursor nuclides of metallic fission products have also to be considered, in particular for Sr-89. It is not clearly known for Cs-137 and Sr-90, to which extent the release of these nuclides is caused by precursors, by formation of contaminated dust due to fuel element erosion and by direct release of the elements or perhaps their compounds. With respect to the Fort St. Vrain HTR there are some indications by diffusion tube measurements, that direct release does not occur and sources of the primary circuit contamination by these nuclides are formation of contaminated dust and gaseous precursors only /58/. In contrast to that, direct release seems to dominate in the AVR reactor /16/; the latter is assumed in actual safety analyses. Sources of this direct release which have to be considered separately are coated particles with intact coatings resp. with

defective coatings and fuel contamination of graphite. Reliable data on the sum of fuel in particles with defective coatings and in graphite are obtained by the fuel element qualification program /15/. The fuel contamination of graphite was continuously decreased by fabrication measures, as shown by separate measurements; new data on single fuel elements indicate a value of $< 10^{-7}$, which however has to be verified for more realistic production conditions and is therefore not considered in tab. II.

It becomes clear from Tab. II, that

- less than $2 \cdot 10^{-4}$ of the inventory is found outside intact coated particles
- the equilibrium activity within the cooling gas is extremly low due to low release from fuel elements and to plate-out on surfaces of primary circuit components
- the inventories of defective particles and of the metallic primary circuit surfaces by plate-out are the largest activities outside in act particles.

3.2 Adsorption on surfaces

Plate-out distribution in the primary circuit is calculated using the codes SPATRA or PATRAS /19/, which combine ad/desorption behaviour and mass-transfer, as first proposed for HTR plate out calculations by Kress and Neill /61/. SPATRA will be explained at first; differences to PATRAS are outlined later (see also App. F). Fig. 5 contains an overview to SPATRA. The ad/desorption equilibrium on metals is given approximately by:

$$p_i = 10^8 \cdot \exp(-\Delta H_{des}/RT) \cdot \sigma/\sigma_0 \quad Pa \qquad (1a)$$

σ= concentration of fission products with respect to the geometrical surface $mol \cdot m^{-2}$

σ_0= monolayer concentration on the geometrical surface $1 \cdot 10^{-5}\ mol \cdot m^{-2}$

ΔH_{des}= desorption enthalpies in the sub monolayer regime $J \cdot mol^{-1}$

R= gas constant = 8.3143 $J \cdot mol^{-1} \cdot K^{-1}$

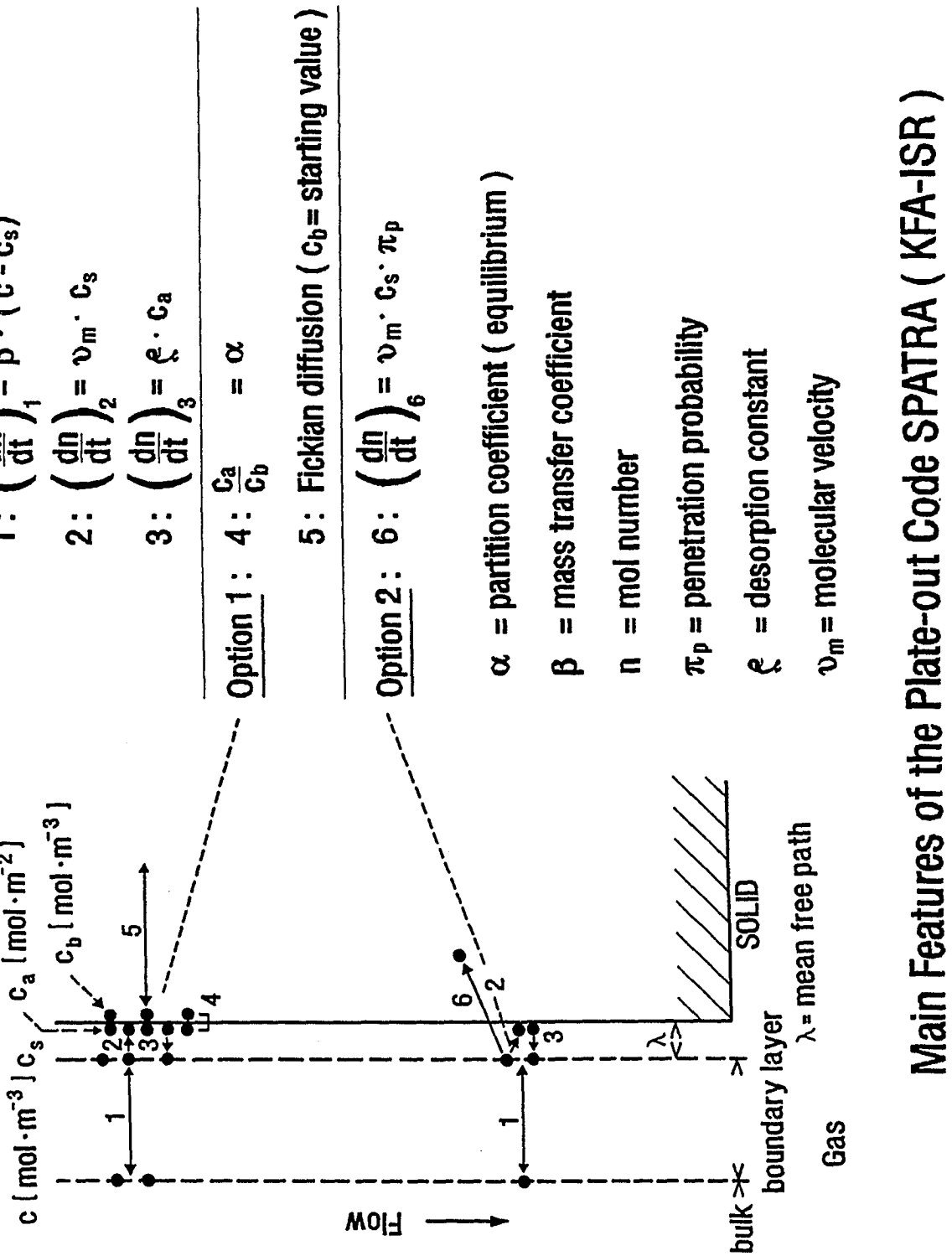

Main Features of the Plate-out Code SPATRA (KFA-ISR)

Fig. 5

Equation (1a) is easily obtained by setting equal the rate of nuclide bumps onto the geometrical surface with the desorption rate (see also Appendix C, eq. C1, which leads for stationary conditions to $c/\sigma = v/\theta$); the latter is proportional to the lattice vibration frequency and to an Arrhenius factor containing the desorption enthalpies. As shown in app. C in detail, the assumption of an ad/desorption equilibrium is reasonable.

Introducing eq. (1a) into the mass transfer equation leads to:

$$d\sigma/dt = \beta/RT \cdot (p_{i,BULK} - 10^8 \cdot \exp(-\Delta H_{des}/RT) \cdot \sigma/\sigma_0) \qquad mol \cdot m^{-2} \cdot s^{-1} \tag{1b}$$

$$\beta = \text{mass transfer coefficient} \qquad m \cdot s^{-1}$$

which has to be solved (in a more complicated form) in SPATRA. Eq. (1b) is valid only for low fission product burden on surfaces, which is usually the case for the normal operating reactor. In case of higher surface concentrations saturation effects have to be taken into account, which means, that fission products cannot be handeled independently with respect to their adsorption behaviour; coverage of effective surfaces near to a monolayer also leads to a significant decrease of desorption enthalpies. However, due to surface roughness, effective HTR surfaces may be at least one order of magnitude larger than the geometrical surfaces.

Desorption enthalpies are about 220-260 $kJ \cdot mol^{-1}$ for cesium and silver and 110-180 $kJ \cdot mol^{-1}$ for iodine, depending on adsorbens and its surface conditions; cesium desorption enthalpies seem to be larger on oxidized surfaces than on clean metallic surfaces, whereas iodine desorption enthalpies are in particular small on oxidized surfaces. A quantitative relation between surface conditions and desorption enthalpies is, however, not available up to now. There are some indications, that cesium desorption enthalpies might be even smaller (160-180 $kJ \cdot mol^{-1}$, s. App. G). One should bear in mind, that the desorption enthalpy influences the sorption isotherms as an exponent; accordingly, the above given data range of $\Delta H_{des}(Cs)$ corresponds to sorption isotherm differences of several orders of magnitude. Strontium plate out behaviour is still less well known; thermochemical estimations reveal, that strontium in presence of oxide layers may be converted into SrO or into another oxidic phase. In that case, eq. (1a) is not applicable and usual vapor pressure equations for pure compounds have to be assumed.

Vapor pressures of oxidic strontium compounds are, however, extremly low. Pure compound vapor pressure equations may also be applied in case of iodine plate out for conditions, where solid FeI_2 formation has to be expected, i.e. only less oxidized metal surfaces at low temperatures /25/. Because of their relevance in particular for source term estimations in water ingress accidents (see chap. 4.3.2) the knowledge concerning desorption resp. vaporization enthalpies for reactor conditions has to be improved by additional experiments.

As an example for SPATRA-calculations, fig. 6 contains experimental /60/ and calculated plate-out profiles of Ag-110m for the in pile experiment VAMPYR-II of the AVR-reactor: In the high temperature part of the specimen, plate-out is controlled by the ad/desorption equilibrium, whereas in the low temperature region mass transfer is dominant. For this case (i.e. nearly constant temperature gradient and experimental parameters constant with time), a first rough evaluation, leading to the desorption constant ϑ for one temperature, is easily possible by linear extrapolations of the mass transfer and the ad/desorption equilibrium lines; for the crosspoint of both lines holds: $\vartheta = v/(\beta \cdot t)$ (with t = experimental time s and v = atomar/molecular velocity $m \cdot s^{-1}$). Desorption enthalpies may than be calculated using the definition of ϑ given in context with eq. (C-1).

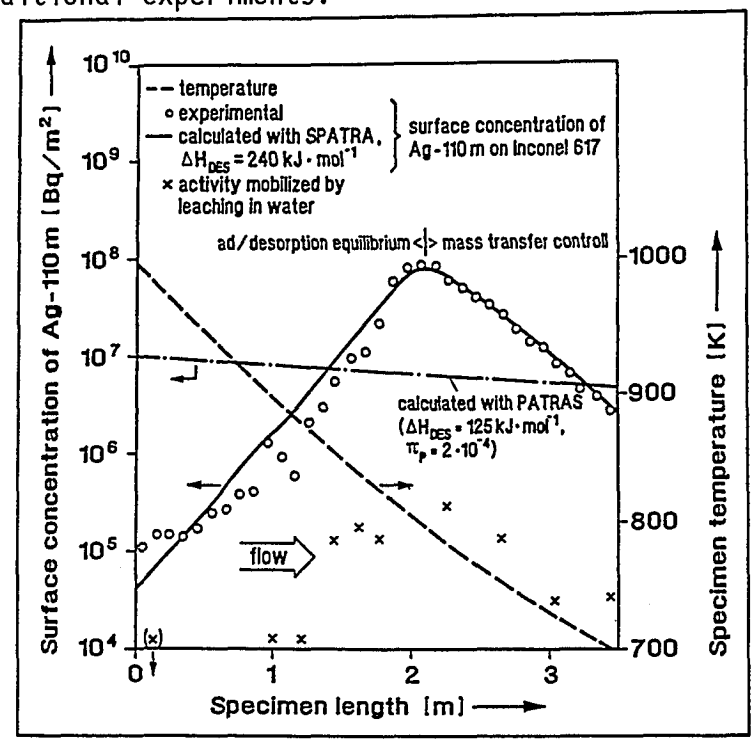

Plate-out experiment - VAMPYR II (AVR): Measured and calculated plate-out profiles for Ag-110m on Inconel 617

Fig. 6

The PATRAS results on Ag-plate out, presented also in figure 6, are discussed in App. F. In the same experiment, cesium plate-out is small and shows a very small temperature dependence; first results of the evaluation of this experiment are discussed in App. G. In the VAMPYR-I experiment /60/ normal plate out curves have been found also in case of cesium on stainless steels; results of evaluations of this experiment

with different models are given in fig. F-1, indicating good agreement for usual SPATRA assumptions. However, the adsorbens metal at least in the high temperature part of this experiment is not representative for the HTR primary circuit high temperature range; in addition, considerable activation processes take place in the high temperature part of VAMPYR-I influencing in particular the Ag-110m concentrations; flow conditions in this loop differ significantly from those in VAMPYR-II.

Iodine plate out in the VAMPYR-I loop is obviously controlled by ad/desorption equilibrium and mass transfer only and is therefore easily handled as fig. 7 indicates. SPATRA-evaluations lead to desorption enthalpies of about 170 ± 15 kJ/mol on 15Mo3. There are some indications from LAMINAR-loop experiments and from other sources, that iodine adsorption might be an activated process under certain conditions. Because of the large time span between plate out phase and postexamination, no iodine data are available from VAMPYR-II.

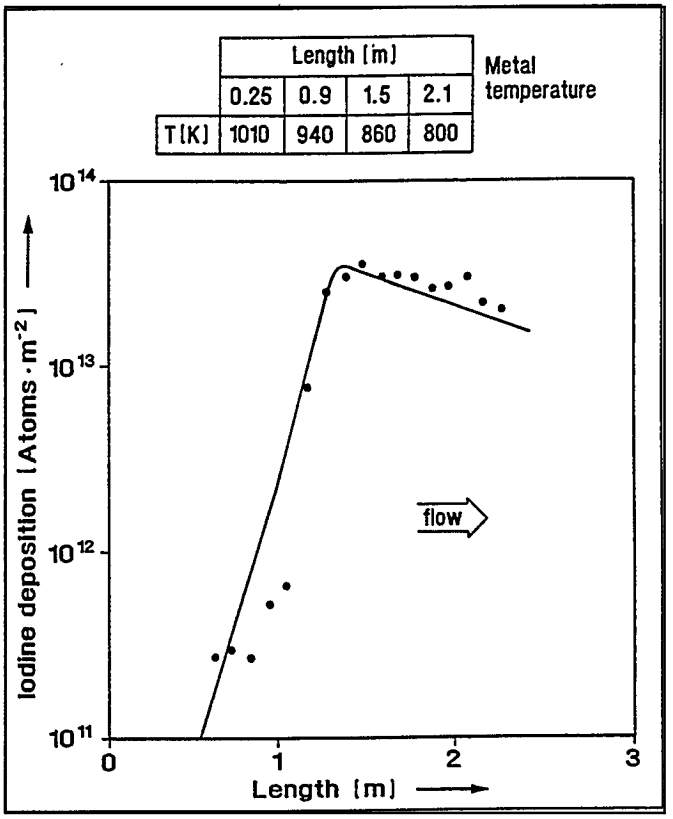

VAMPYR-I-09 :
SPATRA-evaluation of iodine-131 plate-out on 15Mo3 (ΔH_{DES} = 170 kJ·mol^{-1})

Fig. 7

Calculations on the basis of eq. (1b) for the primary circuits of actual HTRs (Peach Bottom /46/, AVR fig. 8 in /48/, /95/) with help of the US codes PAD and PADLOC indicate a sufficient agreement to the measured plate out distribution for Cs-137 and Sr-90 in these reactors. This agreement may be taken as an additional partial validation of the physical plate out model, which is used in a nearly equivalent manner in PAD/PADLOC and SPATRA; besides the arguments in this chapter, other experimental validations for these codes resp. the assumptions on absorption in SPATRA (see next chapter) are given in App. F and G.

3.3 Absorption (Penetration)

SPATRA also contains a simplified model for consideration of absorption processes (see fig. 5): A partition coefficient is assumed between adsorbed and absorbed state; transport within the material is handled as simple Fickian diffusion (option 1). Another option for handling absorption in SPATRA is the penetration coefficient π_p as shortly explained in App. F (resp. option 2 of fig. 5); in option 2 SPATRA does not consider saturation limits for absorption. Absorption effects are experimentally confirmed to some extent for cesium /62/, however, are not well understood up to now: Mechanisms like volume diffusion, diffusion in the micropore or grain boundary system of the oxide layers and growing of oxide layers have to be taken into consideration. Experimental arguments for absorption are: Diffusion profiles of cesium have been found within the oxide/metal layers of metals for a depth of some μm /21,68,69/ at temperatures of 600-800°C = 873-1073 K for diffusion times in the order of some 100 to some 1000 h; in all cases, however, the absolute amount of fission products deeper than the first step of sectioning is very small, indicating, that the absorbed fraction is probably much smaller than the adsorbed fraction. In addition, leaching with water removes only a part of some ten percent of the plated-out cesium /18,62,68/, in particular for high temperature plate out, which might be caused by absorption.

With simple absorption or penetration mechanisms conflicts the following: At temperatures >400°C=673 K the water leach yield shows no clear temperature dependence; if adsorption decreases in favour to absorption with increasing temperatures, as assumed in simple absorption models, a remarkable decrease of the leach yield has to be expected. In addition, diffusion profiles are measured also at low temperatures (<150°C=423 K) and are found not only in mass transfer controlled plate-out regions but also in the ad/desorption controlled branches, the latter sometimes even without showing significant deviations from simple ad/desorption profiles; this might be explained by cesium diffusion along the inner oxide surfaces/grain boundaries with a rate, which is fast compared to the rate constants of cesium desorption into the gas phase. From a physical point of view this is possible, because in case of surface diffusion the cesium atom does not completely leave the attraction range of the surface and corresponding activation energies of diffusion are much smaller than desorption enthalpies. This explanation is compatible with the low leach yield, because penetration of water into the

oxide layer micropore system is strongly impeded. Besides diffusion within the micropore system of the oxide layer, some true absorption (i.e. irreversibility with respect to ad/desorption equilibrium) with cesium inclusion into the metal/oxide volume may occur, too. Absorption hinders remobilization of plated-out fission products; because of its uncertainties, it is conservatively not considered in safety analyses up to now. An overview on models concerning absorption is found in /63/.

A reasonable tool for examination of ad-/absorption effects is the sorption coefficient Γ introduced in /84/. This coefficient is the ratio of actual plate out rate to the maximum rate (controlled by mass transfer) and is easily calculated from plate out profiles. An indication of absorption/penetration is a sorption coefficient significantly < 1 together with a (very) small temperature dependence of that sorption coefficient; in case of simple ad/desorption processes, this combination cannot occur. For a known absorption controlled Γ, the penetration coefficient π_p can easily be calculated by $\pi_p = \Gamma \cdot \beta / v$; this relation is exact for $\Gamma << 1$ (as is usually the case for absorption).

Several plate out experiments have been sometimes interpreted in the past as strongly penetration controlled, although the above given criterion was not fullfilled (e.g. SAPHIR/PEGASE P05 plate out results /85/; this experiment is difficult to examine, because ist contains different metals with different geometrical parameters); in these experiments the sorption coefficient is temperature independent but 1. Such black body behaviour is usually caused by adsorption still far from equilibrium; another reason might be complete inclusion of adsorbed fission products by a very fast growing oxide layer, which however has not to be expected for HTR metals (Incoloy 800, Inconel 617, Hastelloy X for temperatures $\geq 500°C = 773\ K$, several stainless steels like 15Mo3, 4541, 10CrMo910 for lower temperatures) but for titanium (see App. F resp. /77,79/).

As mentioned above the KFA code PATRAS /75/ is very similar to SPATRA with respect to adsorption but considers a temperature independent penetration coefficient (which is identical to the absorption probability of a gas atom bouncing on the surface) and a re-evaporation of the absorbed nuclides if solubility limits are reached. A critical discussion of physical background and data base published for PATRAS is given in App. F. It is shown there, that PATRAS in combination with its data base is not applicable to HTR relevant conditions; however, considering

the penetration coefficient as an empirical factor without a definite physical meaning, and reducing its value by about 2 orders of magnitude in relation to /75/ it is shown, that this model is applicable for rather rough estimations of plate out problems in particular for low fission product concentrations (where the above mentioned solubility limits play no role). This modified penetration model (option 2 of SPA-TRA) is also preferently used in this report, because sufficient input data for the physically more correct option 1 are not available up to now. However, in order to solve the still open questions with respect to absorption, laboratory experiments generating partition coefficients and diffusion data should be performed in future.

3.4 Dust borne activities

Dust borne activities cannot be handled in the moment with a physical model but only on an empirical base; with respect to this empirical handling (s. chapter 4.3.2) it has to be mentioned, that the uncertainties concerning its production, settlement and interaction with gas borne or plated-out activities are high; its activity values in table II are upper limits of the uncertainty scatter and may therefore decrease with increasing knowledge. In connection with dust contributions to the equilibrium cooling gas activities it was found, that an equilibrium like dust concentration within the primary circuit gas is obtained only for very uniform flow conditions, as will be shown in chap. 4.3.2. Basing on experimental evidence from AVR it is assumed, that 10^7 of the overall dust amount within the primary circuit is gas borne under equilibrium like conditions; as will be outlined in chap. 4.3.2 this corresponds in case of the HTR-Modul to about $5 \cdot 10^{-9}$ of the Cs-137 inventory released from core into the primary circuit (or $5 \cdot 10^{-13}$ of the overall reactor inventory). A more detailed description of some calculation methods and data is found in /19/.

3.5 Data base and general estimation guideline

Input for the models for estimation of the fission product distribution at accident initiation are mainly best estimate data of irradiation experiments of fuel elements /15/, of reactor experience /16,17,46,60/ and, in case of plate out, of laboratory experiments, too /18,49,62/. Additional data are expected from a research program at Forschungszen-

trum Rossendorf on 'fission product release in HTR water ingress accidents', where plate out (and remobilization) of Cs and iodine will be measured in a thermogradient tube and in a large plate out loop. One main aim of this work will be the examination of the dependence of plate-out parameters on surface conditions.

Whereas best estimate values of desorption enthalpies in estimations of plate out distributions in safety analyses have to be used, its lower boundaries have to be taken into account in calculations of the equilibrium cooling gas activities; this handling leads to lower limits of the relative plate out per pass respective upper limits of the atomic or molecular cooling gas activities. Because the amount of plate out dominates always for iodine and metals in comparison with the atomic/-molecular gas borne activities, the different handling of gas borne and and plate out does not lead to conflicting mass balances. The equilibrium gas activities of noble gases have to be calculated considering sinks like primary circuit leakages and gas cleaning.

4. MODELS,DATA AND RESULTS OF SOURCE TERM EVALUATION

4.1 Core heat-up events

4.1.1 Coating failure rates

The model PANAMA-I /20/ has been developed in order to calculate the coating failure rates due to temperature increase. This model takes into account the following points:

- internal pressure increase in coated particles by fission gas and CO production
- strength loss of the SiC coating by irradiation and corrosive attack by fission products
- thermal decomposition of SiC, which, however, is important only at temperatures >2073 K=1800°C.

Input data for this code have been obtained from fuel element heating and additional laboratory experiments /20/. Parameter calculations with this code indicate, that besides temperature and time of heating also irradiation temperature history and burn-up determine the coating failure rates. Applying this code to the worst core heat-up events of the HTR-Modul shows, that the amount of temperature induced coating failures remain far below that of failures by fabrication and irradiation.

4.1.2 Fission product transport within the core

The two-dimensional diffusion model FRESCO was developed in order to calculate the fission product release from core. Fickian diffusion is assumed in all components of the fuel element and in the graphitic reflectors; concentration dependent diffusion coefficients, however, may be used. Concerning the small activity inventory in graphite kernels and in the carbon buffer layer of defective particles, a release by diffusion in direction of the internal graphite surfaces is considered only for temperatures < 1523 K=1250°C; for higher temperatures a spontaneous release of this inventory is assumed because of a lack of data. Particles with defective coatings are modelled without coating.

Main input data for FRESCO are temperature and gas flow transients, coating failure rates from PANAMA-I, fission product diffusion coefficients and sorption isotherms of fission products on graphitic materials. An overview on FRESCO and its input data is given in /19/.

A very important result of parameter calculations with FRESCO for core heat-up events of small sized HTRs is, that elemental cesium and strontium, released slightly from hot fuel elements, are nearly totally retained by chemisorption in colder graphitic regions. This remains true, if the experimentally detected deviations from the usually used Fickian diffusion model /70/ are taken into account with respect to the Cs-diffusion in graphite; the latter is explained more detailed in Appendix D. A particular high sorption capability was found for the ungraphitized binder component of the fuel matrix graphite /26/. An validation of the retention model of FRESCO (using a slightly different code) has been performed in /88/ on the basis of Cs-sorption/desorption experiments in flowing argon, loaded with Cs. Due to their high Cs-burden in graphite, a reasonable postcalculation of these experiments required the consideration of concentration dependent diffusion of Cs in graphite, as proposed in /2/. This postcalculation was possible on the basis of input data (diffusion coefficients, sorption isotherms), which have been generated independently in laboratory experiments; solely the relation of activation energy of surface diffusion (within the graphite pores) to sorption enthalpy was not known and fitted to the experimental curve. In contrast to that, the very sucessfull postcalculation with PATRAS-Core (see /88/) does not rely on separately generated data but obviously needs the fit of many parameters.

The extremly high retention in graphite is calculated only for small sized HTRs with its low fission product concentrations in graphite, whereas in medium sized HTRs graphite saturation and chemical reactions like CsI-formation have to be taken into account /24/. Nevertheless, maximum accidental temperatures up to 2273 *K*=2000°*C* might be possible without significant release of cesium and strontium out of the core cavern, if credit is taken on this chemisorption; simply increasing the core diameter, this maximum temperature corresponds to a thermal power of about 600 *MW* /22/. Additional work to this question should be done in future in order to optimize the concept of the HTR-Modul.

Concerning iodine, a limited potential for source term reduction by chemisorption on cold graphitic components exists in small HTRs, as FRESCO calculations using experimental sorption isotherms for the iodine/graphite system indicate. However, the extent of iodine sorption on graphite seems to be strongly influenced by its impurity content /65/; additional measurements are necessary in order to clarify the applicability of iodine sorption isotherms in HTR accidents.

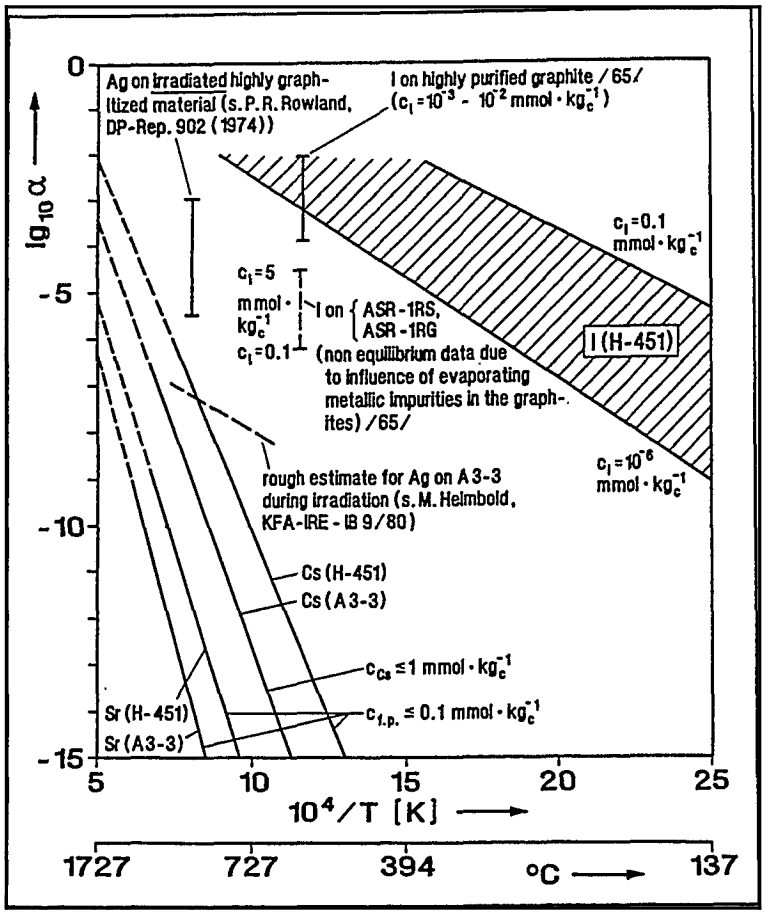

Partition coefficients α of fission products between gas phase and graphite at low concentrations

Fig. 8

Fig. 8 gives an overview on measured equilibrium partition coefficients for certain fission products between gas phase and graphite (Henrian sorption range), demonstrating the high retention capability of graphite.

4.1.3 Temperature induced desorption from surfaces

Models and data used for sorption on graphitic and metallic surfaces (as used in FRESCO resp. SPATRA) can also be applied for calculations of temperature induced desorption. Desorption from graphite has only to be taken into account for the small amount of its iodine content, whereas cesium and strontium are retained by the above outlined chemisorption on cold graphites. Desorption from metal surfaces in particular from the steam generator remains small: Core heat-up does not lead to an overall increase but to an equilization of its temperatures; in most regions with temperature increase the initial nuclide concentrations are far from saturation and, accordingly, heating does not lead to a remarkable desorption.

4.1.4 Representative source terms in core heat-up events

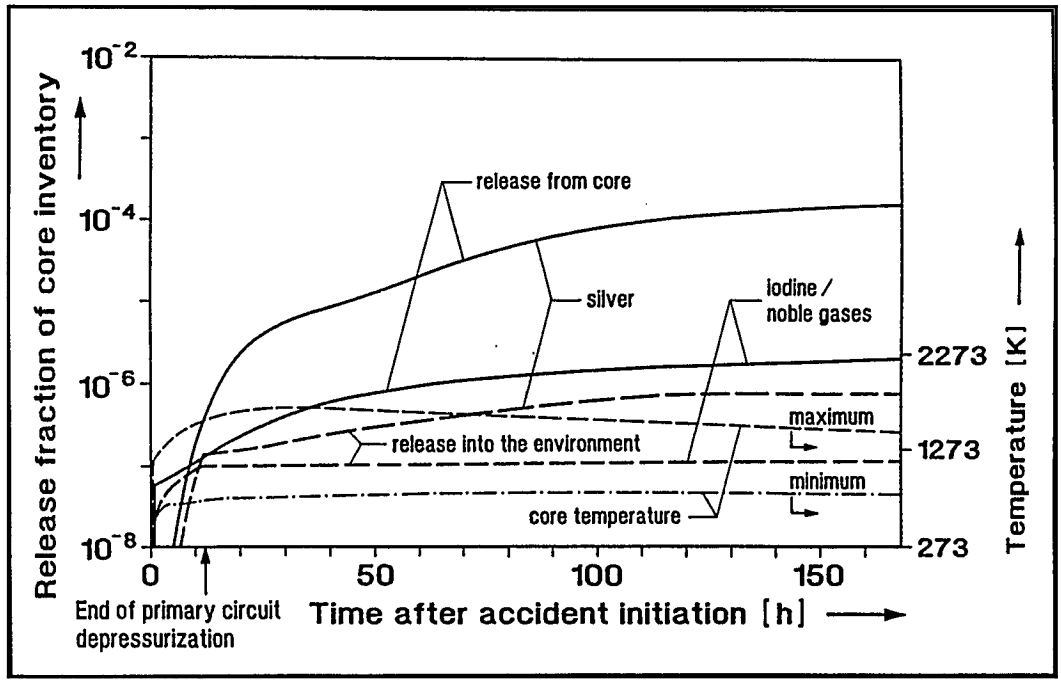

Core heat-up accident in the HTR-Modul following a slow (12h) primary circuit depressurization : Maximum and minimum core temperatures and release fractions from core and into the environment for iodine / noble gases and silver

Fig. 9

In unrestricted core heat-up events of the HTR-Modul fission product release out of the core cavern remains limited to iodine, noble gases and silver, whereas release of cesium and strontium remains far below 10^{-8} of the overall inventory. Fig. 9 contains maximum and average active core temperatures and temperature induced fractional release values out of the core cavern and into the environment for I-131/noble gases and Ag-110m in case of a core heat-up event with slow depressurization /23/; the latter was found to be the worst case concerning release into the environment.

Due to the slow temperature increase, fission product release from core starts late and proceeds slowly. With respect to iodine/noble gases about 15 % of their inventory in defective particles and about 40 % of the graphite kernel inventory are released into the primary circuit, other contributions are negligible. Silver which is not very efficiently retained by coatings or graphite is mainly released from intact particles by diffusion.

Desorption from primary circuit surfaces plays no important role. A reduction of release to the environment occurs due to the buffer effect of the primary circuit volume after depressurization, i.e. the lack of a transport mechanism. The data in fig. 9 do not consider any depletion

along the path into the environment, nor any retention by the reactor building was assumed. Parameter calculations, however, indicate a retention potential for elemental iodine in addition to the above mentioned sorption on graphite: In case of small gas exchange rates between reactor building and environment after completion of depressurization (exchange rates < 0.1 d^{-1}), a significant source term decrease has to be expected by depletion of elemental iodine on building surfaces; the same may hold for silver, too. Iodine converted to organic compounds like CH_3I will not be retained by reaction on building surfaces. An overview on depletion rates of iodine compounds on surfaces is found in /59/.

4.2 Water and air ingress accidents

4.2.1 Release from defective coated particles

Attack of oxidants on UO_2 in steam and limited air ingress accidents is restricted to particles with defective coatings. It leads to an hyperstoichiometric oxide UO_{2+x} /27,40/; in course of that oxidation, a part of the fission product inventory on intergranular bubbles and grain boundaries may be released; in addition, diffusion coefficients of fission products within the oxide grains increase. These release mechanisms mainly affect iodine and noble gases; there are, however, some indications, that also cesium release might be influenced /28/.

The equilibrium degree of uranium oxidation is determined by the local oxygen potential, which strongly depends on the graphite oxidation processes: Consumption of oxidants decreases the oxygen potential within the fuel element and, additionaly, in case of steam ingress accidents H_2 and CO formation significantly diminishes that potential. The first step of release estimations is therefore the calculation of the oxygen potential within the fuel zone of fuel elements during accidents; this is done with help of the code COROX /29/, which calculates graphite oxidation influenced diffusion profiles of the oxidants and of their reaction products in the porous graphite and also estimates the profile of the corrosion degree. Typical concentration profiles of steam, hydrogen and oxygen in a fuel element at 900 °C = 1173 K are shown in fig. 10 for steam ingress; corresponding equilibrium oxidation degrees of fuel are given too. In this case, the equilibrium hyperstoichiometric coefficient x remains < 0.003 due to the low oxygen potential within the fuel element; this low oxygen potential is here

mainly due to hydrogen formation and not to consumption of steam. For a similar case without graphite oxidation, i.e. pure steam in helium, the equilibrium hyperstoichiometric coefficient x would reach values ≥ 0.6, which corresponds to an oxygen partial pressure of 0.1 *Pa*.

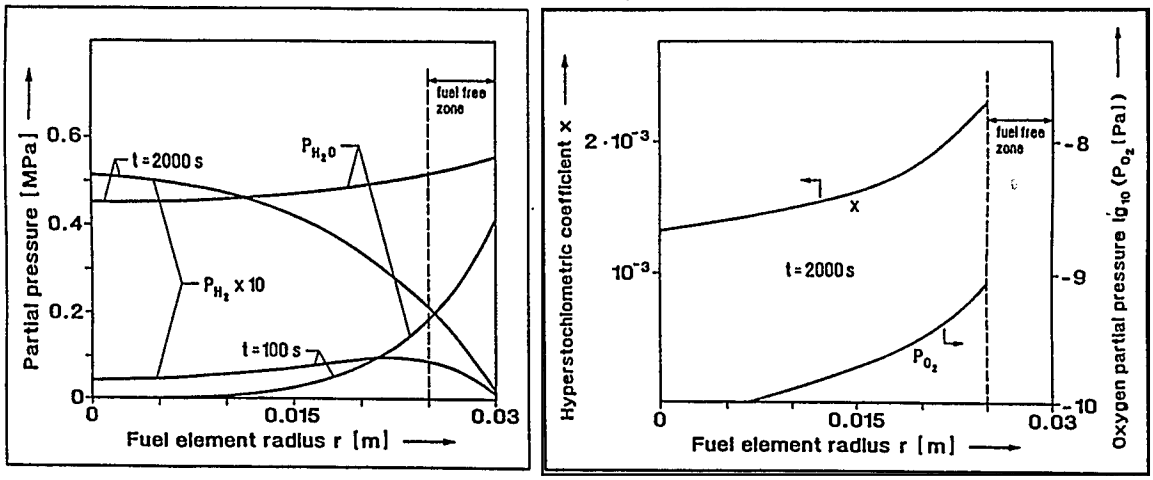

a. Profiles of steam and hydrogen partial pressure

b. Partial pressure of oxygen and corresponding hyperstochiometric coefficient x in uranium oxide (UO_{2+x})

Oxidation behaviour of UO_2 in defective particles of an HTR fuel element in steam/He mixtures (T: 1173 K ≙ 900 °C, P_{total} = 7.5 MPa)

Fig. 10

In general, high graphite oxidation rates are coupled with low penetration of oxidants into the graphite and vice verse. Significant rates with penetration depth of < 5 *mm* are found for the oxygen/graphite reaction at temperatures >650°*C*=923 *K* and for the steam/graphite reaction at temperatures >1050 °*C*=1323 *K* (ambient pressure) resp. at >1000°*C* = 1273 *K* (normal operation pressures of HTRs); these temperatures may be taken as upper limits, which is conservative with respect to UO_2-oxidation. Considering, that coated particles are embedded only in the inner part of the fuel elements (s. fig. 1), a remarkable fuel oxidation by air is therefore possible only at temperatures below 650°*C*=923 *K*; in case of steam, the strong influence of hydrogen on the oxygen potential leads to an additional reduction of the upper temperature limit to about 750°*C*=1023 *K*.

Concerning oxidation kinetics of UO_2 it is a well known fact, that chemical diffusion rates of oxygen in fuel are very high /30/; a kinetic hindrance of oxidation may therefore not to be expected, provided, the oxidation process on the geometrical fuel surface proceeds sufficiently fast. The latter seems to be the case for air attack on fuel, but not necessarily for steam; very slow UO_2 oxidation kinetics in steam at 600°*C*=873 *K* /31/ indicates, that surface kinetics (or perhaps gas phase kinetics of steam dissociation) are rate limiting steps

at low temperatures, whereas at high temperatures (>1023°C=1300 K) chemical diffusion controlled rates are found /32/. In accident analyses it is assumed with concern to kinetics, that air oxidation of fuel is limited by chemical oxygen diffusion at all temperatures, whereas sufficiently fast steam oxidation is supposed to take place only at temperatures >600°C=873 K, then also limited by chemical oxygen diffusion; the assumptions for steam ingress might be rather conservative.

There is a significant lack of knowledge with respect to the fission product release induced by this fuel oxidation in particular for high burn-up fuel. Sufficient knowledge exists only for the increase of in-grain diffusion coefficients of iodine and noble gases due to oxidation, which is in the order of a factor of 100 for $UO_{2.10}$ /33/. In contrast, the fraction of short lived nuclides within intergranular bubbles and grain boundaries and its release by oxidation is not well known. Heating of high burn-up fuel kernels equipped only with porous buffer layers up to 1600°C=1873 K indicates, that the inventory outside of UO_2 grains is <1.5 % for I-131 /34/; the recoil inventory within the buffer, however, was not separable from bubble/grain boundary inventory. In accident calculations concerning fuel oxidation it is conservatively assumed, that the latter inventory fraction is 1.5 % of the overall particle inventory, i.e. the buffer inventory is neglected here. It is further postulated, that the release of the fuel inventory outside grains is proportional to the hyperstoichiometric coefficient x and is total at x=0.2; the latter is roughly estimated from release transients of irradiated hyperstoichiometric uranium oxides /35/. Additional experiments on steam attack on irradiated fuel elements containing defective particles, will be executed in KFA/IRW in order to improve the knowledge in this area and to reduce conservatisms. Experiments on the oxidation kinetics of UO_2-kernels in steam/H_2 at T > 300°C = 573 K have to be performed at Forschungszentrum Rossendorf using a solid state coulometric method /86/; first results indicate a substantial kinetic hindrance /87/. Important work on oxidation induced fission product release from coated particles has been done in USA, too /91/, in particular for UCO kernels.

Applying the above outlined model on severe steam ingress accidents of the HTR-Modul, it was found, that iodine and noble gas release fractions out of defective particles and into the environment remain below $3 \cdot 10^{-7}$ of the overall inventory. Release calculations for limited air ingress accidents have not yet been executed; a noteworthy air ingress

into the core of the HTR-Modul in case of 1 small leak in the primary circuit enclosure is possible only in continuation of a core-heat up, i.e. when the primary circuit cools down and air is sucked in by contraction. For this scenario it may be supposed, that release into the primary circuit due to fuel oxidation is remarkably higher than during steam ingress accidents, the negligibly small gas transport out of the primary circuit, however, prevents any significant release into the environment.

4.2.2 Release from graphite

Release from graphite may occur due to direct interaction between the fission products in graphite and water, steam or oxygen, or due to gasification of graphite together with its fission product content. Concerning the graphite grain inventory, only the second mechanism is possible, because at least its main part cannot be reached by oxidants.

With respect to the inventory on inner surfaces, thermochemical equilibrium calculations indicate, that graphite oxidation by steam is preferred in relation to oxidative Cs- or Sr-gasification /36/. This was confirmed by experiments with steam attack on graphite, containing cesium, strontium and silver, without, however reaching significant degrees of graphite corrosion: Only CO and H_2 were detected in the gas phase but no fission products. The same holds for oxygen attack, too, as theoretical considerations indicate.

The protection of the chemisorbed metals due to graphite corrosion by steam may not be considered at low temperatures (< 750°C= 1023 *K*) because this graphite oxidation does not take place for kinetic or thermochemical reasons; however, also under these circumstances, a significant vaporization of cesium sorbed on graphite does not take place, as the equilibrium constant K_2 of the reaction

$$Cs...C + H_2O \rightarrow CsOH_g + 0.5\ H_2\ (+C) \qquad (2)$$

on matrix graphite indicates (for thermochemistry of Cs..C s. /24/):

$$K_2 = p°_{CsOH} \cdot p°_{H2}{}^{0.5} / p°_{H2O} \qquad (3)$$

$$= c_C \cdot \exp(-44700/T+7.78)$$

$$p°_i = p_i / p_0 \quad p_0 = 0.1013\ MPa \quad c_C < 1\ mmol_{Cs} \cdot kg_C^{-1}$$

These calculations do not take into account an interaction between gaseous CsOH and steam, which is known to exist at high steam pressures; as outlined in detail in App. B, this interaction may lead to an enlargement of K_2, which, however, does not change that result in general. A conversion of sorbed cesium into a $CsOH_s$ phase is possible from a thermochemical point of view only for small H_2/H_2O-ratios and high temperatures; in case of sorbed strontium a reaction to $Sr(OH)_{2,s}$ is more favourized. In any case, such oxidations do not increase the release of cesium or strontium from graphite.

Another experiment on oxidation induced release on graphite (steam attack) reveals, that release of chemisorbed strontium remains much less than the corrosion degree of the graphite /37/; an explanation to this might be, that strontium migrates deeper into the graphite instead of beeing gasified because of the high stability of its chemisorbed state. The latter result, however, has conservatively not taken into consideration in safety analyses up to now.

Attack of liquid water is expected to mobilize a larger part of the chemisorbed metallic fission products than steam: This is because ionic metals solvated in water are more stable than in gaseous compounds. The (sorbed) cesium dissolution reaction is endothermic (85 $kJ \cdot mol^{-1}$ on A3-matrix, Henrian sorption). Penetration of water into graphite pores is a slow process as experiments indicate; in addition, some sorption of Cs^+ or Sr^{2+} may occur in presence of liquid water. Nevertheless, in safety analyses is assumed, that chemisorbed metallic fission products in wetted graphite regions are completely dissoluted in water.

Concerning the small amount of (weakly) sorbed iodine, which is found only in low temperature regions with slow graphite oxidation kinetics, a mobilization due to steam, water and air has to be expected; because of the low iodine sorption enthalpies, displacement adsorption may also play a role in this mobilization. Also, a complete mobilization during steam/water attack has to be assumed for sorbed tritium due to an exchange reaction; however, from a radiological point of view tritium plays no dominant role.

The above outlined mobilization kinetics has to be interferred with fission product distribution in graphite and with penetration of oxidants/corrosion into the graphite. Concerning the latter, the above mentioned code REACT/THERMIX (s. chap. 2.2), which also includes chemical reactions between steam and graphite, is used for estimation of the global graphite corrosion and temperature transients, whereas local

penetration profiles are obtained by COROX (s. chap. 4.2.1). With respect to oxidation of matrix graphite, one should bear in mind, that its ungraphitized binder content is preferently oxidized. For fission product distribution within the graphite the following is assumed: Fission products, sorbed in the low temperature core regions from the gas phase, concentrate near to outer geometrical surface of the graphite, as AVR-data indicate /38/; in hot regions, the distribution of sorbed fission products is more homogeneous. As mentioned in chap. 4.1.2, fission products sorbed in fuel matrix graphite are found mainly in its binder content, which amounts to about 10 weight-% of the material and is homogeneously distributed in it. Caused by uranium diffusion during high temperature treatment in fuel element production, there should be a higher concentration of the graphite grain inventory of fission products in the surroundings of particles, defective from fabrication; the activity due to the natural uranium contamination of matrix graphite is equally distributed. The oxidation induced release fractions of local inventory from reflector graphite is assumed to be equal to its degree of oxidation and with concern to the sorbed inventory of the fuel matrix graphite to the corrosion degree of its binder content.

Parametric accident analyses indicate, that < 0.1 % of the graphite inventory in the core cavern of an HTR-Modul will be gasified in water/steam ingress accidents and a still smaller amount in (limited) air ingress accidents. Taking that into account, the release from graphite in water or air ingress accidents does not exceed 10^{-7} of the overall core inventory of radiological important nuclides.

4.2.3 Release of fission products plated out on metal surfaces

4.2.3.1 Mobilization by liquid water

Thermochemical equilibrium considerations indicate, that attack of liquid water nearly quantitatively dissolves cesium and strontium, plated out on metallic/oxidic surfaces (wash off); cesium plate out data of /18,62/ (ΔH_{des}=234 $kJ \cdot mol^{-1}$) lead to the following equilibrium for chemisorption in the sub-monolayer regime on Incoloy 800 in presence of liquid water:

$$Cs..M + H_2O \rightarrow CsOH_{solv} + 0.5\ H_2 \qquad (4)$$

$$K_4 = [CsOH] \cdot p°_{H2}{}^{0.5} = \exp(5410/T+3.62) \cdot \sigma/\sigma_0 \qquad (5)$$

[ ] molality $mol \cdot kg^{-1}{}_{solution}$

σ/σ_0 fractional coverage of geometrical surface with cesium

This wash off reaction is slightly exothermic (-45 $kJ \cdot mol^{-1}$). The same must not be true for silver because of its noble character; the sorption characteristics of silver on metals, outlined in fig. 6, with sorption enthalpies similar to the sublimation enthalpy of the element (=270 $kJ \cdot mol^{-1}$) also points out, that silver sorption is more like a physisorption; i.e. its elemental character remains probably unchanged. Measurements of silver leaching indicates, that about 1% of its plated out amount is dissolved (s. fig. 6). Nevertheless, also a silver dissolution of 10 % is conservatively assumed in recent safety analyses. A total dissolution is postulated for iodine because of its comparably low sorption enthalpy (s. chap. 3) and its complex chemical behaviour in liquid solution.

Leaching experiments at 25-90°C (=298-363 K) indicate, that a kinetic hindrance of dissolution with time constants of some minutes exists /18,39,62/; similar to the behaviour in graphite, this may be caused by slow transport of water into the micropore system of oxide surface layers. This kinetic hindrance is not taken into consideration in safety analyses, in particular, because water temperatures in accidents are much higher than in experiments and because of the bad knowledge with respect to the actual localization of sorbed fission products within the oxide layer/metal.

Besides dissolution and chemical attack of liquid water on sorbed fission products, also mechanical (erosive) effects due to a high speed water jet in course of a tube rupture have to be taken into consideration; it is conservatively assumed, that the directly impacted surface (some m^2) is completely decontaminated.

The fission product content of liquid water may be released mainly by (fast) evaporation of the water (bubbling and droplet formation), volatilization of the residue after complete water evaporation and transport of the gas borne activity into the environment. In addition, an equilibrium partition between steam and liquid water has to be assumed, which is influenced by solubilities in steam, as quantified in App. B. In our HTR safety analyses it has been conservatively postulated up to now, that the dissoluted fission products are transferred into the gas phase proportional to the degree of water evaporation. There are some indications, however, that this might be a significant overprediction /41/, at least for metallic fission products. High gas flow rates with significant water suspension may have the same effect as evaporation.

Data on Cs and iodine wash-off will be generated within the next years at Forschungszentrum Rossendorf as part of the above mentioned research program.

4.2.3.2 Mobilization by steam or air attack

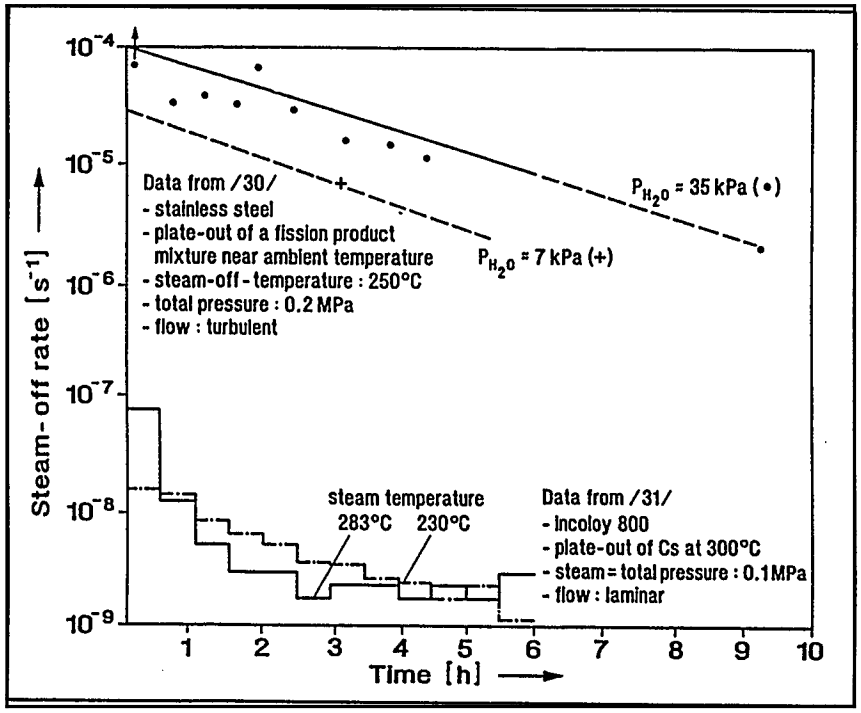

Release rates for cesium, plated-out on metals, during steam attack (steam-off)

Fig. 11

There are only a few experimental data on removal of chemisorbed fission products from metals by an attack of steam (steam off) or air. In addition, the data scatter is remarkably high, as fig. 11 for cesium indicates; this figure contains two sets of measurements on steam off rates for cesium on HTR relevant metals, showing rate differences of 4 orders of magnitude and more.

Thermochemical estimations lead to the following equilibrium relationships for cesium steam off on Incoloy 800:

$$Cs..M/O + H_2O_g \rightarrow CsOH_g + 0.5H_2 \qquad (6)$$

$$K_6 = p°_{CsOH} \cdot p°_{H2}{}^{0.5} / p°_{H2O} = \sigma/\sigma_0 \exp(-16750/T - 4.42) \qquad (7)$$

The reaction enthalpy of (6) is endothermic with about 139 $kJ \cdot mol^{-1}$. For conditions as in fig. 11 (250°C=523 K, $p°_{H2O}$=0.5), with the assumptions that $p°_{H2}=0.001 \cdot p°_{H2O}$, the equilibrium partial pressure of CsOH is calculated to be in the order of $4 \cdot 10^{-10} \cdot \sigma/\sigma_0$ Pa; an additional increase by $CsOH_g$/steam interaction has not to be expected in these conditions, as may be obtained by using data of App. B. In comparison with values of eq.(1a) that means an increase of cesium containing species in the gas phase in equilibrium by more than 6 orders of magnitude due to the presence of steam; if chemisorption of steam or hydrogen on

sorption sites previously occupied by cesium is taken into account too (displacement adsorption), an additional increase has to be expected, which cannot be sufficiently quantified because of a lack of data. A still higher increase occurs also, if oxidation of metallic sorption sites proceeds simultaneously to the chemical conversion of cesium. However, mass transfer in combination with the still small partition coefficient between gas and chemisorbed phase significantly limits the relative steam off rate τ; provided sorption is -as usually assumed- an unactivated process, the ad/desorption step itself cannot be a rate limiting factor, i.e. a spontaneous ad/desorption equilibrium on the surface/gas boundary has to be expected (s. App. C) and is considered in the following equation:

$$\tau = \beta \cdot p_{CsOH}/(RT \cdot \sigma) \qquad s^{-1} \qquad (8)$$

One should bear in mind, that in eq. (8) $p_{CsOH,BULK}$ is assumed to be zero which leads to an upper limit of the mass transfer rate for a given equilibrium partial pressure. Mass transfer coefficients for laminar flow in tubular geometry are in the order of 0.01 $m \cdot s^{-1}$, which leads with the above given $p_{CsOH}=4 \cdot 10^{-10} \cdot \sigma/\sigma_0$ *Pa* to relative steam off rates of $1 \cdot 10^{-10}$ s^{-1}, i.e. a value just below the lower boundary of that, found in /39/ (s. fig. 11). This underestimation of the measured steam off rate might be caused by uncertainties in experimental desorption enthalpies: A decrease of the desorption enthalpy by 5 % increases the relative steam off rate by more than one order of magnitude. In this context it should be noted, that evaluation of VAMPYR-II (s. App. G) leads to desorption enthalpies, which are about 25 % smaller than the data of the LAMINAR-loop, used in (7). Also, uncertainties in mass transfer coefficients and hydrogen partial pressure might contribute to these deviations. The interpretation given in /39/ for their steam off data, leading to the somewhat surprising result of decreasing steam off rates with increasing temperatures, is not applicable in safety analyses without a convincing experimental validation.

The drastically higher steam off rates of /42/ also shown in fig. 11 are partially caused by a larger mass transfer coefficient in these experiments; the latter may be responsible for an increase of not more than 2 orders of magnitude. Another rate increasing factor might be a lower sorption enthalpy of cesium on that stainless steel due to its composition and surface conditions or due to a fission product burden near to its saturation limit; in addition, displacement adsorption or

metal oxidation, as outlined above, might play here a role in steam off acceleration. The significant uncertainties in this field require additional experiments: Besides measurements on steam off rates carefull determinations of the desorption enthalpies (i.e. the thermochemical status of the sorbed cesium) are necessary. This will be done in future in the research program at Forschungszentrum Rossendorf mentioned above. An algorithm based on eq. (8) should be included in the plate out code SPATRA, allowing for estimations of accidental steam off.

In safety analyses, the above outlined calculation method will be used for estimation of steam off rates for cesium; in order to consider the uncertainties in chemical behaviour, in particular the above mentioned influence of displacement adsorption/adsorbens oxidation, a safety factor of 1000 should be applied on the equilibrium partial pressure of CsOH. For strontium and silver, the cesium steam off rates reduced by a factor of 0.1 will be used. This procedure seems to be highly conservative in particular for strontium: As explained in chapter 3 its chemical state on oxidized metal surfaces is probably not only a chemisorbed one but an oxidic phase with volatilities, which remain very low also when interaction of its gaseous phase with steam is taken into consideration (s. App. B). The lack of experimental data with respect to strontium, however, forces this handling.

Cesium mobilization by dry air is small because of the low stabilities of cesium oxides in comparision with CsOH; in air with natural moisture content, the reaction

$$2\ Cs..M/O + 0.5\ O_2 + H_2O_g \rightarrow 2\ CsOH_g \qquad (9)$$

is highly favourized, as outlined in detail in App. A. For strontium and silver in air, a similar handling as that in steam has to be applied.

Iodine does not form compounds in reaction with steam or air which are significantly more stable than the element. On the other hand, its chemisorption enthalpies are low and release by displacement adsorption of H_2O or oxygen resp. adsorbens oxidation might be possible. Evaluation of iodine mobilization in steam/air mixtures indicates /25/, that at temperatures >160°*C*=433 *K* a total mobilization has to be expected. Experiments in Helium containing 3000 *Pa* H_2O show, that iodine desorption rates at 300°*C*=573 *K* increase by about a factor of 20 in comparison with pure Helium /43/; the dependence of the desorption rate on

flow velocity found in these experiments leads to the conclusion, that mass transfer within the boundary layer is rate determining and not partition kinetics between gas and solid. Accordingly, the rate increase factors probably reflect also the change in equilibrium; this change will probably be proportional to the steam partial pressure, which has to be considered in safety analyses, too. Because iodine and steam sorption enthalpies may depend on surface conditions in a different manner, a higher increase for other surface conditions than in these experiments may be expected; therefore, an additional safety factor of 5 has to be assumed on the above given experimental data, which leads to the following relation between sorption isotherms in dry and moist Helium:

$$p^{\circ}_{I,moist} = p^{\circ}_{I,dry} \cdot (1. + 3500 \cdot p^{\circ}_{H2O}) \qquad (10)$$

These isotherms have to be combined with mass transfer correlations in a similar manner as shown above for cesium in steam. One should bear in mind, that this handling of iodine steam off contains significant conservatisms, which should be diminished by additional experiments. An indication for conservatisms may be found in results of the AVR water ingress /44/: The above given model postulates a nearly complete steam off of iodine for that accident, whereas only about 15 % of the steam generator contamination were found within the water, removed from the primary circuit. Reliable data on iodine steam-off at temperatures up to 400°C are expected from the research program at Forschungszentrum Rossendorf. Inserting p°_{O2} instead of p°_{H2O}, eq. (10) may be used for calculation of iodine mobilization by air, too.

4.2.3.3 Exemplaric source term contributions caused by mobilization of plate out activity

During water ingress accidents in small HTRs, a mobilization of some percent of the steam generator inventory may be transferred into the gas phase by wash off and subsequent water evaporation; steam off of iodine may be complete at least for steam attack durations in the order of hours. Steam off of metallic fission products remains however limited to some percent of the steam generator contamination in the time up to the end of depressurization. Release of this mobilized activity (fractions of the overall inventory for Cs-137:$<5 \cdot 10^{-6}$, I-131: $<2 \cdot 10^{-7}$) into the environment is between 10% and complete for relevant scenarios

of the HTR-Modul. Usually, these water ingress contributions determine the risk of small HTRs.

Mobilization by oxygen during (limited) air ingress is at most in the same range as by steam; transport into the environment, however, remains very small, because air ingress -as mentioned above- starts not earlier than after completion of primary circuit depressurization.

4.3 **Depressurization events**

4.3.1 Desorption of plate-out activity due to pressure drop

If an ad/desorption equilibrium is assumed for all gas/surface interlayers of the primary circuit, a pressure change Δp leads to an increase of the molecular gas borne equilibrium activity by a factor f_p:

$$f_p = \ln(p_s/(p_s-\Delta p)) \cdot p_s/\Delta p \qquad (11)$$

p_s=system pressure at depressurization start

SPATRA calculations however indicate, that in typical HTR normal operation conditions most of the plate out proceeds mass transfer controlled, i.e. the surfaces act as a nearly complete sink and surface concentrations are far from equilibrium. This may also be seen from fig. 6, showing plate out curves for the AVR experiment VAMPYR-II including the regimes of mass transfer control and ad/desorption equilibrium. Nevertheless, because of the comparably small increase of the extraordinary low molecular fission product concentration in the cooling gas by a pressure drop (f_p<5), eq. (11) is used in safety analyses, giving an upper limit of the molecular contribution to the depressurization source term.

4.3.2 Lift off of dust borne activity

As outlined in chapter 3.4, the uncertainties with respect to dust are remarkably high. In pebble bed HTRs most of the dust seems to be produced by friction of fuel element pebbles in particular in the fuel handling system; accordingly, it consists mainly of carbon. In addition, some metallic dust is found (Fe and its alloy partners) and metal oxides were observed, too. Also cracking of oil impurities and carburization may play a role in production of some small sized dust. The AVR reactor contains about 60 *kg* of dust after 20 *y* of operation,

as was estimated from results of dust filtering experiments in its hot and cold gas regions.

With respect to dust depletion in normal operation two different effects have to be considered: On the one hand dust transport to surfaces mainly by turbulent diffusion and sticking by adhesion and on the other hand sedimentation of (preferently larger) dust particles in dead water regions.

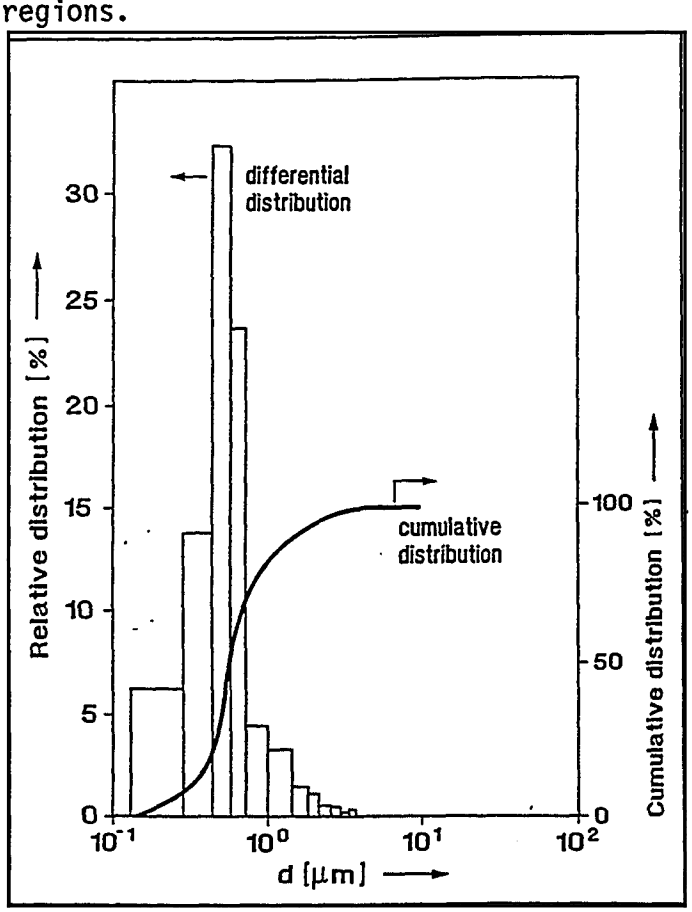

Typical (number weighted) distribution of dust particle diameters in the AVR primary circuit (dust from VAMPYR-I filters, experiment V 41)

Fig. 12

It is a well known fact, that adhesive bounded particles of a diameter of < 50 μm are not easily removed by shear forces /45/. The average size of AVR dust seems to be significantly smaller as a typical distribution of particle numbers given in fig. 12 indicates /46,60/; its average diameter of about 0.6 μm corresponds to a median diameter of about 5-10 μm in case of a particle volume weighted distribution. The size distribution of AVR dust seems to be similar for all filter experiments. One should bear in mind, however, that an agglomeration of individual dust particles on surfaces, leading to particle sizes which can be easier lifted off by depressurization induced shear forces cannot be excluded in particular for high dust concentrations. Adhesive bounded dust may change the plate out behaviour of primary circuit surfaces.

Sedimented dust may be partly lifted off in case of fast depressurizations; this may be also concluded from AVR experiments with blower transients, whose results are shown in fig. 13: Changing the flow rate leads to an increase of the gas borne dust (which is in equilibrium with < 5 $\mu g \cdot Nm^{-3}$ very low) by up to 3 orders of magnitude /47/. The in-

crease is probably due to flow disturbances during the change of the flow rate; accordingly, when these disturbances are gone, the increase of dust concentration vanishes by depletion within some hours as fig. 13 indicates. Flow disturbances have also to be expected in course of or preceeding to depressurization events.

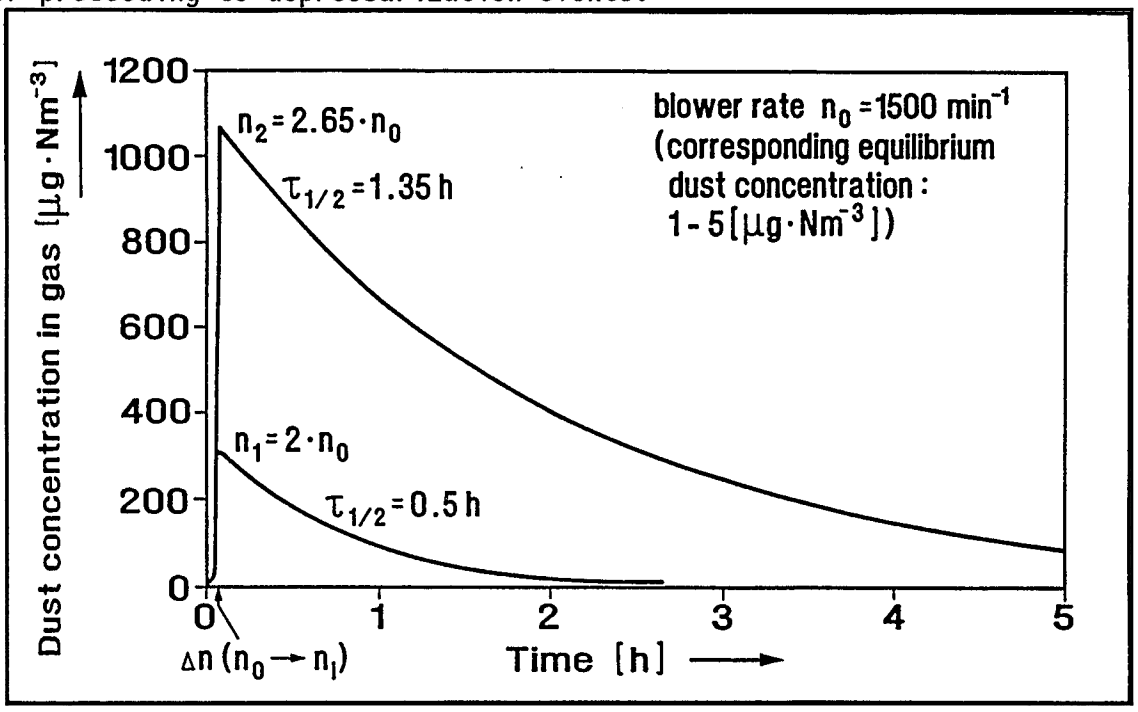

Transient dust concentrations in the AVR primary gas following fast changes of the blower rate n
Fig. 13

With respect to the dust borne activity in AVR, it was estimated from filter experiments, that dust contains about 10 % of the amount of Cs-137 and Sr-90 released out of the core cavern in normal operation /48/. Because of the much smaller dust amount expected for modern HTR concepts like the HTR-Modul, in particular due to dust filtering in the fuel element handling system, the dust borne fraction of the primary circuit activity is assumed to be smaller in the HTR-Module by a factor of about 5 for these nuclides, as tab. II (chap. 3.1) outlines. Significant activities of Ag-110m were also found in the AVR dust /48/, whereas its I-131 content was thought to be nearly negligible in the past; however, recent on-line examination of dust during the blower transient experiments indicated, that the activity concentration of I-131 in the AVR-dust mobilized during the transient reaches values of up to 3.5 $GBq \cdot kg^{-1}$; considering, that the integral value of iodine in the AVR primary circuit is in the order of 25 *GBq* and the overall amount of dust is about 60 *kg*, this means, that iodine is inhomogeneously distributed on the dust content of the primary circuit and that in partic-

ular such dust, which contains large concentrations of iodine, is mobilized during transients. The reason for this is probably, that the outer layers of the sedimented dust, which come easily in contact with the gas flow, are equilibrated with fission products; due to nuclear decay, there will be a concentration decrease in direction to deeper, earlier settled dust layers, particularly for short lived nuclides. The outer dust layers seem to be a preferent object of mobilization. There are no quantitative information about the activity gradient within the settled dust and so, the dust borne fraction of the radiological important iodine nuclides cannot be quantified so far.

It is important to note, that examination of dust specimens removed by wiping from AVR primary circuit surfaces shows remarkable differences with concern to specific activities of long lived nuclides /48/: In particular dust from fuel element surfaces has a significant smaller specific activity then dust depleted or adhesive bound on primary circuit components. This was confirmed by postexamination of irradiated AVR fuel elements: Specific activities on fuel element surfaces /38/ are 1 to 2 orders of magnitude smaller than dust activities /48/. Assuming, that dust formation proceeds mainly by friction of fuel elements this leads to the conclusion, that it is not sufficient to consider the activity content on fuel element surfaces as a source of the dust activity: Interaction of dust with molecular gas borne or plated out activity has also to be taken into account. This, however, is difficult to correlate with another observation in the AVR: Dust from dead water regions measured during blower transients has roughly the same specific activity as adhesive bound dust, i.e. much higher activities than found on fuel element surfaces; a remarkable additional (long lived) fission product loading of dust in deep water regions is hardly to imagine because of the small mass transfer efficiency in this area. The latter observation can obviously be explained only by the assumption of a (slow) particle exchange between areas with sedimented and adhesive bound dust during reactor normal operation. Perhaps local flow turbulencies like that proposed in /67/ in combination with the above mentioned growing of adhesive bound particles by agglomeration are responsible for such an activity exchange. These interpretations are, however, highly speculative and cannot be a basis of accident calculations.

In AGRs similar experiments as in AVR have been executed /50/: At first, flow increase by a factor of 2 led to an increase of gas borne

Fe-59, Co-58 and Mn-54 by about 4 orders of magnitude; these nuclides are assumed to be mainly fixed on dust. In addition, dust particles of 2, 5 and 17 μm diameter labelled with Fe-59 have been injected into the primary circuit. The dependence of depletion and remobilization behaviour on dust diameter allows some conclusions on physical mechanisms: Impaction of dust on surfaces seems to be one important depletion mechanism, which however is reduced by bouncing-off; the latter is proportional to particle size and to flow rate. Adhesion sites on the surfaces show a broad distribution of interaction energies with the dust particles due to surface inhomogenities; this causes remobilization and redepletion of particles until energetic favourable sites are found.

Besides the above outlined plant experience there are some other data on dust borne activity in gas cooled reactors: In laboratory experiments with graphite dust containing (comparably high concentrations of) strontium it was shown, that in course of dust depletion on hot preoxidized metal surfaces most of the strontium moves within a day into the metal oxide layer, in particular in regions with high Cr_2O_3 content; in case of temperatures < 500°C=773 K this transfer occurred to a smaller extent /55,56/. Further these experiments indicate, that dust preferently sticks on clean metallic surfaces, whereas adhesion forces on oxidized surfaces seem to be weaker; a lift off of the dust particles (diameter 50-100 μm) by flow rate increase has been observed. The latter, however, is not representative for HTR dust because of the comparably large size of the dust used in these experiments. Cesium shows a similar but not as pronounced behaviour as strontium in graphitic dust.

Lift off experiments have also been executed in the french COMEDIE-loop /51/. The specimens used in these experiments were taken from the Peach Bottom HTR with block core; dust of these reactor types shows usually another characteristics /52/ than dust from pebble bed HTRs and therefore, these results may not been directly applied to the latter. The COMEDIE experiments indicate a strong dependence of lift-off from surfaces on the shear force ratio: For shear forces smaller than in Peach Bottom normal operation no or only slight releases have been detected. Increasing the shear forces beyond values of Peach Bottom normal operation leads to a significant lift off, which is in the order of some percent of the total (i.e. not only of the dust) inventory of cesium, strontium and cobalt on the metallic surfaces in case of a shear force ratio of 2. There was no clear distinction between dust and plate out

activity in these experiments. Similar experiments will be performed in future as part of the US-MHTGR program in the COMEDIE-loop and in the (out of pile) DABLE-loop at MIT (Boston).

The comparably high lift off in the COMEDIE experiments rises the question, whether a surface erosion with dust formation may occur in course of HTR primary circuit depressurizations; such erosion could lead to a partial lift off of the plated out activity, too. With concern to this question some cesium plate out and desorption experiments in the KFA loop SMOC should be mentioned; these experiments also included variation of the mass flow /53/. In contrast to COMEDIE no significant lift off was observed in case of flow rate increase. The amount of dust in SMOC is, however, believed to be very small.

Experiments have been performed also with respect to dust settlement in dead water regions behind a step /54/; graphitic dust particles of an average diameter of 50 μm have been used. Additional experiments indicate that settled dust is partly lifted off in case of a reversion of the flow direction.

Summing up the above outlined experience on dust and lift off, there is no sufficient physical based assessment available up to now which allows dust treatment in HTRs. Substantial research work is necessary in order to obtain a better understanding of the dust behaviour.

In actual safety analyses it is supposed, that the adhesive bonded dust borne activity is equally distributed over all surfaces of the primary circuit; because adhesion forces tend to be only slightly temperature dependent, this assumption will not be so much in error, provided, that the surface structure within the primary circuit is roughly homogeneous. The amount of adhesively bonded dust is roughly assumed to be one half of the total amount of dust; the other half is considered to be sedimented dust. AVR-data are basis for the values of the dust borne fraction of the overall activity in table II; these values consider for long lived nuclides a smaller relative dust production rate in the HTR-Modul in comparison with the AVR due to a dust filter in the refuelling system. Sufficient corresponding AVR-data for iodine do not exist, as explained above; the relative iodine sorption capacity of dust is roughly assumed to be 50 % of that of the long lived metals. This value consideres the weaker iodine sorption on graphite on the one hand, but its strong sorption on metallic dust components on the other hand. A reduction of the dust borne fraction of iodine due to the smaller dust formation rates in modern HTRs compared with the AVR is not taken into

account for short lived nuclides because their interaction with dust seems to be restricted to the gas-side dust layers.

In case of a depressurization, all dust in areas with shear forces greater than in normal operation conditions is predicted to be lifted off. In order to take into account the release of dust settled in dead water regions by sedimentation it is additionaly assumed, that 1 % of this dust inventory is lifted off in case of those depressurizations, for which flow disturbances in dead water areas during the or preceeding to the depressurization cannot explicitely be excluded; this value is at least by a factor of 5 larger than observed in experiments with blower transients (AVR, CAGR) but was chosen because of the still bad knowledge with respect to lift off of settled dust. Considering the activity concentration in the dust settled by sedimentation it is assumed, that long lived nuclides are equally distributed, whereas short lived iodine isotopes are conservatively supposed to be completely sorbed in the mobilized dust fraction.

Part of the adsorbable activity entering the gas clean-up plant is sorbed there on dust particles, e.g. dust sticking on filters. In safety analyses it is assumed, that a fraction of 20 % of all adsorbable activities reaching the clean-up plant are dust borne at the beginning of a depressurization accident. These inventories, whose absolute values also depend on the cleaning capacity of the particular clean-up plant, become important in depressurizations with fast, reverse flow in the clean-up plant (e.g. depressurization via a leak in that plant).

4.4.3 Source terms in depressurization events

The amount of I-131 which may be released during a (dry) primary circuit depressurization of the HTR-Modul without dust mobilization is in the order of 0.02 *GBq*. In case of accidents with mobilization of sedimented dust in the primary circuit and complete blown out of the dust inventory of the gas clean-up plant the I-131 release into the environment was conservatively estimated to 2 *GBq* and the Cs-137 release to 0.4 *GBq*; the contribution of dust from the clean-up plant dominates the Cs-137 source term (contribution of about 80 %), but remains negligible for iodine. A significant release of adhesive bonded dust is not expected for depressurizations with leak diameters in the primary circuit

enclosure of ≤ 0.065 *m* (refuelling tube diameter), because shear forces in most primary circuit areas are below that of normal operation conditions. Larger leaks are much less frequent due to design measures. The contribution of these small source terms to the overall risk of the HTR-Modul is significant because of the comparably high frequency of these events.

5. CONCLUSIONS

Source term evaluations for small sized HTRs have to consider core heat-up events, depressurizations, water- and air ingress into the primary circuit and reactivity transients. For core heat-up accidents the design of this reactor type excludes temperatures significantly beyond $1600°C = 1873\ K$; on the basis of a reliable knowledge with respect to source term models and data the release of radiological important fission products under these conditions remains restricted to $< 10^{-6}$ of the overall inventory for iodine and noble gases and to $< 10^{-8}$ for cesium and strontium. Research work which could probably allow for an additional reduction of these already low source terms. Temperature induced fission product release in this reactor type is therefore severely limited. Reactivity transients are apparently covered by core heat-up events.

Quantitative source term evaluations for the other important accident types partly suffer on still high uncertainties with respect to release models and data; however, except possibly for unlimited air ingress (which is a highly hypothetical event), these accidents cannot lead to a release of that predominant fission product fraction which is enclosed in particles with intact coatings (>99.98 % of the overall fission product inventory); in addition, also for most cases with high uncertainies the upper limit of release may be further significantly diminished by the model assessments and data presented in the preceeding chapters. Accordingly, these uncertainties cannot call in question the generally high safety features of small HTRs. Nevertheless, in order to obtain reliable quantitative results with respect to the safety features of this reactor type some additional research work is necessary: In particular the behaviour of dust borne fission products, the fission product plate out and remobilization and the release of fission products in course of UO_2-oxidation by steam or air have to be considered in detail.

Concerning plate out it became clear, that the penetration (absorption) mechanism is much less important than assumed sometimes in the past.

6. LITERATURE

/1/ R.Moormann, K.Verfondern: Estimation of severe accident source terms for HTGR's: State of the art. IAEA-SM-296 (1988), vol. 1, p.449-460

/2/ R.Moormann, K.Röllig: Spaltproduktfreisetzung bei HTR-Störfällen. Proceedings of Fachsitzung 'Stand der HTR-Sicherheitsforschung', Jahrestagung Kerntechnik '89, (1989) p.64-87

/3/ J.Ehrhardt et al.: The program system UFOMOD to assess the consequences of nuclear accidents. KfK-4330 (1988)

/4/ Incident calculation bases for the guidelines issued by the BMI for the assessment of the design of PWR nuclear power plants pursuent to § 28.3 of the radiological protection ordinance (18.10.1983). Translation safety codes and guides; editor: GRS Quantitative examinationts Cologne.

/5/ Rahmenempfehlungen für den Katastrophenschutz in der Umgebung kerntechnischer Anlagen. GMBl 40 (1989) 71

/6/ H.Reutler, G.H.Lohnert: Advances in going modular in HTRs. Nuclear Eng. Design 78 (1984) 129-36

/7/ W.Schenk, H.Nabielek: Kugelbrennelemente mit TRISO-Partikeln bei Störfalltemperaturen. Jül-Spez-487 (1989)

/8/ K.Verfondern, W.Schenk, H.Nabielek: Passive safety characteristics of fuel for modular HTR and fuel performance modeling under accident conditions. Nuclear Techn. 91 (1990) 235-46

/9/ W.Jahn, W.Rehm: pers. communication

/10/ G.H.Lohnert, T.Kindt, W.Scherer: Das Verhalten des HTR-Modul bei Reaktivitätsstörfällen. Proceedings of Fachsitzung 'Stand der HTR-Sicherheitsforschung', Jahrestagung Kerntechnik '89, (1989) p.26-47

/11/ Zum Störfallverhalten des HTR-100. Ed.: J.Mertens, Jül-Spez-477 (1988)

/12/ R.Moormann, W.Katscher: Examination on graphite 'burning' in HTGR's. Proc. 2th symp. on nucl. reactor sev. accident chem., Toronto 1988, (in press)

/13/ R.Moormann, K.Petersen: REACT/THERMIX ein Rechenprogramm zur Ermittlung der störfallbedingten Graphitkorrosion in Hochtemperaturreaktoren. Jül-1782 (1982)

/14/ T.Ogawa, K.Fukuda, K.Shiba: HTGR fuel behaviour under accident conditions. Proc. JAERI-GKAE Seminar on fuel element and fuel composition of HTGR, Tokyo 20.-22.10.1987, p.3/81-99

/15/ W.Heit, H.Huschka, W.Rind, G.Kaiser: Status of qualification of High-Temperature Reactor fuel element spheres. Nucl.Techn. 69 (1985) 44

/16/ U.Wawrzik, G.Ivens: Operational monitoring of the release behaviour of the AVR core. Proc. IAEA spec. meet. on fission product release and transport in GCR, Gloucester (1985), IWGGCR/13 (IAEA 1986) p. 15-26

/17/ K.P.Stewart: Final summary report on the PEACH BOTTOM end of life program. GA-A-14404 (1978)

/18/ K.Röllig, A.Christ, F.W.Haase, J.Wiedmann: Cesium deposition on HTR primary circuit materials. Proc. IAEA spec. meet. on fission product release and transport in GCR, Gloucester (1985), IWGGCR/13 (IAEA 1986) p. 329-50

/19/ R.Moormann, K.Verfondern: Methodik umfassender probabilistischer Sicherheitsanalysen für HTR-Anlagenkonzepte; Band 3: Spaltproduktfreisetzung. Jül-Spez-388/3 (1987)

/20/ K.Verfondern, H.Nabielek: PANAMA ein Rechenprogramm zur Vorhersage des Partikelbruchanteils von TRISO-Partikeln unter Störfallbedingungen. Jül-Spez-298 (1985)

/21/ Hj.Matzke, S.Pickering: Diffusion of cesium in stainless steel and possible implications for Cr depletion and mobility. J.Nucl.Sci.Techn. 20 (1983) 237-45

/22/ U.Fricke: Untersuchungen zur Leistungssteigerung von inhärent sicheren HTR durch Optimierung der Coreauslegung. Jül-2155 (1987)

/23/ K.Verfondern, D.Müller: pers. communication

/24/ R.Moormann, K.Hilpert: Chemical behaviour of fission products in core heat-up accidents in High-Temperature Gas-Cooled Reactors. Nucl. Techn. 94 (1991) 56-67

/25/ E.Hoinkis: A review of the adsorption of iodine on metal and its behaviour in loops. ORNL-TM-2916 (1970)

/26/ K.Hilpert, H.Gerads, D.Kath, D.Kobertz: Sorption of cesium and its vaporization from graphitic materials at high temperatures. High Temp.-High Press. 20 (1988) 157-64

/27/ T.B.Lindemer, T.M.Besman: Chemical thermodynamic representation of $UO_{2\pm x}$. J.Nucl.Mat. 130 (1985) 473-88

/28/ G.Falta, G.Reitsamer: Freisetzung fester Spaltprodukte aus bestrahlten HTR-Brennstoffkernen bei Raumtemperatur nach Abtrennung der Teilchenbeschichtung. Part 1: CH-262/80 (1980), Part 2: CH-263-80 (1980)

/29/ G.Meister: COROX ein Rechenprogramm zur Simulation von Wasser- und Lufteinbrüchen in HTR. KFA internal report to appear

/30/ W.Breitung: Oxygen self and chemical diffusion coefficients in $UO_{2\pm x}$. J.Nucl.Mat. 74 (1978) 10-18

/31/ W.C.Kuhlmann: Treatment of UO_2 with water vapor at high temperatures. MCW-103 (1948)

/32/ J.T.Bittel, L.H.Sjodahl, J.F.White: Steam oxidation kinetics and oxygen diffusion in UO_2 at high temperatures. J.Am.Ceram.Soc. 52 (1969) 446-51

/33/ J.B.Lewis: Fundamental aspects of defective nuclear fuel behaviour and fission product release. J.Nucl.Mat. 160 (1988) 201-17

/34/ W.Schenk, D.Pitzer, H.Nabielek: Fission product release profiles from spherical HTR fuel elements at accident temperatures. Jül-2234 (1988)

/35/ K.Shiba: Fission iodine and xenon release from the UO_2-U_3O_8 system with emphasis on radiation damage. J.Nucl.Mat. 57 (1975) 271-9

/36/ R.Moormann: Untersuchungen zum chemischen Verhalten der Spaltprodukte bei HTR-Kernaufheizstörfällen. Proc. Jahrestagung Kerntechnik 1985, München, p.163-66 (ISSN 0720-9207)

/37/ Publ. serv. comp. of Colorado 330 MW HTGR R&D program, quart. progress rep. for the period ending sept. 30, 1966. GA-7453 (1967) p.127-8

/38/ G.Ivens, M.Wimmers: Der AVR als Testbett für Brennelemente. VDI-Ber. 729 (1989) p.161-76

/39/ N.Iniotakis, C.B.von der Decken: Radiological consequences of a depressurization accident combined with water ingress in an HTR Modul-200. Nuclear Eng. Design 109 (1988) 299-306

/40/ Hj. Matzke: Gas release mechanisms in UO_2 - a critical review. Radiation effects 53 (1980) 219

/41/ R.Borkowski, H.Bunz, W.Schöck: Resuspension of fission products during severe accidents in LWR's. KfK-3987 (1985)

/42/ GCR program semiann. progress rep. for the period ending sept. 30, 1966. ORNL-4035 (1967) p.124-6

/43/ GCR program ann. progress report 1973. ORNL-4975 (1975) chap. 13

/44/ F.P.O. Ashworth: Information from water ingress accident on AVR. Jül-Spez-43 (1979)

/45/ W.C.Hinds: Aerosol Technology, chap. 6, NY (1982)

/46/ D.L.Hanson, N.L.Baldwin, D.E.Strong: Fission product behaviour in the Peach Bottom and Fort St. Vrain HTGR's. IWGGCR/2 (IAEA 1981) p.49-54

/47/ U.Wawrzik, P.Biedermann, H.F.Oetjen: Staub im AVR-Reaktor; Verhalten bei transienten Strömungsbedingungen. Proc. Jahrestagung Kerntechnik 1988, Travemünde, p.171-74 (ISSN 0720-9207)

/48/ U.Wawrzik, C.B.von der Decken: Staub- und Aktivitätsverhalten. VDI-Ber. 729 (1989) p.239-54

/49/ D.L. Hanson: Results of the General Atomic deposition loop program. GA-A 13140 (1976)

/50/ J.A.Garland, A.C.Wells, E.J.Higham, I.C.Smith: Experimental study of the deposition of iodine and other fission products in a coolant circuit of a CAGR. Proc 5th int. meet. thermal nucl. reactor safety 1984, Karlsruhe 1984, KfK-3880 (1984) p.1423-31

/51/ R.J.Blanchard, A.Bros, J.Gentil: Out-of-pile Helium loop for liftoff experiments. IWGGCR/2 (IAEA 1981) p.19-25

/52/ F.F. Dyer, R.P.Wichner, W.J.Martin, H.J. de Nordwall: Distribution of radionuclides in the Peach Bottom HTGR primary circuit during core 2 operation. ORNL-5188 (1977)

/53/ N.Iniotakis, C.B. von der Decken, H.Dederichs, B.Sackmann: Verhalten von Spaltprodukten bei der Simulation von Druckentlastungsstörfällen im Kreislauf SMOC. Proc. Jahrestagung Kerntechnik 1983, Berlin, p.219-22 (ISSN 0720-9207)

/54/ R.Griemert: Staubablagerung in Gebieten abgelöster Strömung. Jül-1985 (1985)

/55/ Publ. serv. comp. of Colorado 330 MW HTGR R&D program, quart. progress rep. for the period ending sept. 30, 1967. GA-8270 (1967) p.141-3

/56/ Publ. serv. comp. of Colorado 330 MW HTGR R&D program, quart. progress rep. for the period ending june 30, 1968. GA-8725 (1968) p.99-101

/57/ H.G.Heitmann: Fundamental research in the field of water chemistry in power plants during the last years and its demands. Proc. 9thInt. Conf. Prop. Steam 1979, (1980) p.533-46

/58/ R.D.Burnette: Analysis of the first plateout probe from the Fort St. Vrain HTGR. Trans. Am. Nucl. Soc. 46 (1984) 379-80

/59/ E.C.Beahm, W.E.Shockley C.F.Weber: Chemistry and transport of iodine in containment. Proc. Int. Symp. on Source Term Eval. for Accident Cond., Columbus (OH) 28.10.-1.11.1985, p. 479-500

/60/ P.Biedermann, B.Sackmann: Labor- und Reaktorversuche zur Ablagerung von Spaltprodukten im HTR-Primärkreislauf. Jül-Conf-64 (1988) p. 72-87 (ed. F.Scholz)

/61/ T.S.Kress, F.H.Neill: A model for fission product transport and deposition under isothermal conditions. ORNL-TM-1274 (1965)

/62/ A.Christ, F.W.Haase, J.Wiedmann: Experimentelle Untersuchungen zur Cäsium-Ablagerung auf Hochtemperatur-Werkstoffen. Proc. Jahrestagung Kerntechnik 1985, München, p.175-8 (ISSN 0720-9207)

/63/ J.Herion: Der Einfluß der Wandmaterialien auf die Ablagerung von Cs in HTR-Kühlkreisläufen. Jül-1155 (1975)

/64/ K.Verfondern, D.Müller: Code development for fission product behavior in HTR fuel for safety assessments. KFA internal report ISF-IB-10/89 (1989)

/65/ A.Schoofs: Die physikalischen Grundlagen der Absorption und Desorption von Jod in Reaktorgraphit. Diploma thesis, RWTH Aachen (1989)

/66/ J.Wolters, R.Bongartz, W.Jahn, R.Moormann: The significance of water ingress accidents in small HTRs. Nuclear Eng. Design 109 (1988) 289-94

/67/ G.Skryme: Attachment of gaseous fission products to aerosols. Proc. IAEA spec. meet. on fission product release and transport in GCR, Gloucester (1985), IWGGCR/13 (IAEA 1986) p. 262-74

/68/ K.Hammeke: Experimentelle Ergebnisse der Ablagerungs- und Diffusionsmessungen von Spalt- und Aktivierungsprodukten beim Bestrahlungsexperiment Saphir 11. Internal report KFA-IRB-IB-22/83 (1983)

/69/ I.Petersen: Zusammenstellung aller experimentellen Ergebnisse der Plate-out Untersuchungen an dem Gasführungsrohr des KFA-Heißgasisolierungsexperiments im DRAGON-Reaktor. Internal report KFA-IRB-12/84 (1984)

/70/ H.Gauss, W.Hensel, E.Hoinkis, D.Stritzke: Untersuchungen zum Cs-Transport in Graphit. HMI-B 315 (1979)

/71/ Protection of the Public in the Event of Major Radiation Accidents: Principles for Planning. ICRP-40 (1984)

/72/ NUKEM-83007 (1983); Internal report

/73/ J.Fassbender et al.: Ermittlung von Strahlendosen in der Umgebung des THTR-300 infolge eines angenommenen Coreaufheizunfalls. Jül-Spez-275 (1984)

/74/ H.U.Brinkmann, V.Maly, W.R.Cox, L.R.K.Richard: Burner off-gas examination in the volume reduction experiment on spent HTR-fuel at AEE Winfrith. Proc. Jahrestagung Kerntechnik '86, Aachen 8.-10.4.1986, p. 313-6

/75/ N.Iniotakis: Aktueller Stand der Theorie und der Datei auf dem Gebiet von plate out bei KFA-IRB; in ZFK-747 (1991), p. 389 ff

/76/ Hj.Matzke, S.Pickering: Diffusion of cesium in stainless steel and possible implications for Chromium depletion and mobility. J.Nuc.Sci.Techn. 20 (1983) 237-45

/77/ R.L.Wooley: The deposition of Caesium from a gas coolant II. RD/B/N4787 (1980)

/78/ M.Saito, T.Matsuura, H.Furuya: Diffusion of cesium in stainless steel. J.Nuc.Sci.Techn. 18 (1981) 206-11

/79/ R.L.Wooley: Adsorption/Absorption characteristics of Caesium on oxidized stainless steel. J.Chem.Soc., Farad.Trans. 74 (1978) 1420-34

/80/ J.J.Abassin, R.J.Blanchard, J.Gentil: In pile loop 'COMEDIE': IWGGCR/2 (IAEA 1981) p. 8-18

/81/ A.Christ, K.Röllig, ABB/HRB Mannheim, personal communication 28.3.1988

/82/ D.Schreiber, Siemens-INTERATOM, personal communication 25.3.1988, 1.6.1988

/83/ P.Biedermann, H.Blick, Th.Lennartz, J.Seifert: Technical notes on Postexamination of VAMPYR-II; KFA-IRB TN-10-87, TN-08-89, TN 03-91.

/84/ B.K.Bylkin, I.M.Ibragimov, A.A.Khrulev: Diffusional deposition of fission products in HTGR's. Atomnaya Energiya 67 (1989) 323-6 (transl. in Soviet Atomic Energy)

/85/ N.Iniotakis, J.Malinowski, K.Münchow: Initial results of investigations into fission product deposition in in-pile experiments. Nucl.Eng.Des. 34 (1975) 169-80

/86/ K.Teske: HT-Reaktionen von Oxiden und Mischoxiden; in ZFK-747 (1991), p. 382-3

/87/ C.Nebelung: Untersuchungen von Kernbrennstoff-Wasser-Reaktionen mit Feststoff-elektrolytmeßtechnik; in ZFK-747 (1991), p. 384-5

/88/ L.Kranz: Spaltproduktransport im Hochtemperaturreaktor; Jül-2463 (1991)

/89/ D.W.Hill, B.F.Myers: Temperature, pressure and oxidation effects on cesium diffusion in H-451 graphite; Proc. 16th Bien. Conf. Carbon, July 18-22 (1983) San Diego (USA), p. 556-7

/90/ A.Müller: STADIF-II, ein Programm zur Berechnung der stationären Kühlgasaktivität in Kugelhaufen-HTR. Jül-1464 (1977)

/91/ B.F.Myers: Analysis of the HRB-17 and -18 experiments; ORNL-TM-11169 (1989)

/92/ K.Sawa, O.Baba: The verification of fission products plate out code for HTGR PLAIN; JAERI-M-91-084 (1991)

/93/ R.Moormann, G.Meister: Spaltproduktablagerung auf Metallen und der Code SPATRA; in ZFK-747 (1991) p.56-60

/94/ Patent DE 2655310 C3 (1982): Filter zur Reinigung eines strömenden Gases von einer als atomare oder molekulare Teilchen vorliegenden Substanz.

/95/ Pretest analyses in support of AVR depressurization program. GA Inc., San Diego (USA), Draft Report DOE-HTGR-88120 (1988)

/96/ N.Iniotakis, C.B.von der Decken, K.Röllig, H.J.Schlesinger: Plate-out of fission products and its effect on maintenance and repair. Nucl.Eng.Des. 78 (1984) 273-84

7. LIST OF SYMBOLS

b = emission coefficient from traps s^{-1}

c = concentration in gas $mol \cdot m^{-3}$

c_C = concentration in graphite $mol \cdot m^{-3}$

c_D = concentration on diffusion sites $mol \cdot m^{-3}$

D = diffusion coefficient $m^2 \cdot s^{-1}$

D_{eff} = effective diffusion coefficient $m^2 \cdot s^{-1}$

K_i = thermochemical equilibrium constants

m = concentration on traps $mol \cdot m^{-3}$

p° = p/p_0 with p_0 = 0.1013 MPa (thermochemical standard pressure)

R = gas constant = 8.3143 $J \cdot mol^{-1} \cdot K^{-1}$

v = molecular velocity $m \cdot s^{-1}$

x = hyperstoichiometric coefficient of Uraniumdioxide

β = mass transfer coefficient $m \cdot s^{-1}$

ΔG = free enthalpy $J \cdot mol^{-1}$

ΔH = enthalpy $J \cdot mol^{-1}$

Φ = volumetric molar rate $mol \cdot m^{-3} \cdot s^{-1}$

μ = trapping coefficient s^{-1}

τ = time constant s^{-1}

ϑ = desorption constant s^{-1}

π_p = penetration coefficient

σ = surface concentration $mol \cdot m^{-2}$

σ_0 = concentration of a monolayer on the geometrical surface
$\approx 10^{-5}$ $mol \cdot m^{-2}$

Appendix A: THERMOCHEMICAL EQUILIBRIA IN AIR INGRESS ACCIDENTS: FISSION PRODUCTS PLATED OUT ON METALS

Concerning cesium plate out on Incoloy 800, the following reactions

$$2\ Cs..M/O + 0.5\ O_2 \rightarrow Cs_2O_g \qquad (A1)$$

$$Cs..M/O + 0.5\ O_2 \rightarrow CsO_g \qquad (A2)$$

are nearly impossible during air ingress, as their equilibrium constants indicate (plate out data taken from /18,62/):

$$K_{A1} = 0.285 \cdot (\sigma/\sigma_0)^2 \cdot \exp(-26940./T) = p°_{Cs2O}/\sqrt{p°_{O2}} \qquad (A3)$$

$$K_{A2} = 41.1 \cdot (\sigma/\sigma_0) \cdot \exp(-26540./T) = p°_{CsO}/\sqrt{p°_{O2}} \qquad (A4)$$

(773 *K* = 500°*C*: $K_{A1}=2.1\cdot10^{-16}\cdot(\sigma/\sigma_0)^2$, $K_{A2}=5\cdot10^{-14}\ \sigma/\sigma_0$)

This is mainly due to the low thermochemical stability of the gaseous cesium oxides. In case of presence of moisture, the reaction

$$2\ Cs..M/O + 0.5\ O_2 + H_2O \rightarrow 2\ CsOH_g \qquad (A5)$$

is highly favourized:

$$K_{A5} = 0.132 \cdot (\sigma/\sigma_0)^2 \cdot \exp(-8035./T) = p°_{CsOH}{}^2/(p°_{H2O} \cdot \sqrt{p°_{O2}}) \qquad (A6)$$

(773 *K* = 500°*C*: $K_{A5}=4\cdot10^{-6}\cdot(\sigma/\sigma_0)^2$)

Except for very low air/moisture concentrations, a significant cesium mobilization by moist air attack has therefore to be expected.

Appendix B: SOLUBILITY OF FISSION PRODUCT COMPOUNDS IN STEAM AND ITS INFLUENCE ON THEIR THERMOCHEMICAL DATA

It is a well known fact, that vapor pressures of ionic compounds are significantly higher in high pressure steam than in inert atmospheres /57/. This is mainly caused by an interaction between the polar steam and the ions, probably similar to a solvation in liquid solutions. With respect to important fission product compounds like CsOH or SrO there are no data on solubility in steam available up to now. However, for chemical related compounds like NaOH and BaO, partition coefficients between high pressure steam (1-22 *MPa*) and liquid solution have been measured; a compilation considering all available data up to 1978 is found in /57/. Measured partition coefficients for NaOH and BaO are:

$$K_{NaOH}=p°_{NaOH}/[NaOH]=8.0\cdot10^{-22}\cdot p°_{H2O}{}^{8.5} \qquad (B1)$$

$$K_{BaO}=p°_{BaO}/[BaO]=1.5\cdot10^{-11}\cdot p°_{H2O}{}^{4.5} \qquad (B2)$$

A temperature dependence of this partition is not given in /57/, although a decreasing partition coefficient with increasing temperatures might be expected from a theoretical point of view. These partition coefficients should therefore not be used far outside of the temperature range of the corresponding experiments (200-400°*C*=473-673 *K*). The chemical form of BaO in steam and in liquid solution is probably $Ba(OH)_2$. In the following calculations it is assumed, that the partition coefficients for NaOH are applicable for CsOH and the data for $Ba(OH)_2$ may be used for $Sr(OH)_2$. With respect to CsOH this might lead to an overprediction of the steam solution effect, because Cs^+ is not as good solvated as Na^+ due to its large ionic radius. Ionic radii of Ba^{2+} and Sr^{2+} are more similar; a slight underprediction of the steam solubility of $Sr(OH)_2$, however, might occur by adaption of barium data.

Comparing partition coefficients of CsOH and $Sr(OH)_2$ between liquid solution and inert gas with that of eq. (B1) and (B2) leads to free excess enthalpies of the beforementioned compounds in steam:

$$\Delta G_{ex,CsOH} = \Delta G_{CsOHg,wet} - \Delta G_{CsOHg,dry} \qquad (B3)$$

$$= -RT\cdot\ln\{8.\cdot10^{-22}\cdot p°_{H2O}{}^{8.5}+\exp(-27530./T+16.31)\}$$

$$-228900.+135.6\cdot T \qquad J\cdot mol^{-1}$$

$$\Delta G_{ex,Sr(OH)2} = \Delta H_{Sr(OH)2,g,wet} - \Delta G_{Sr(OH)2,g,dry} \qquad \text{(B4)}$$

$$= -RT \cdot \ln\{1.5 \cdot 10^{-11} \cdot p°_{H2O}{}^{4.5} + \exp(-49170./T + 42.29)\}$$

$$-408800. + 351.6 \cdot T \qquad J \cdot mol^{-1}$$

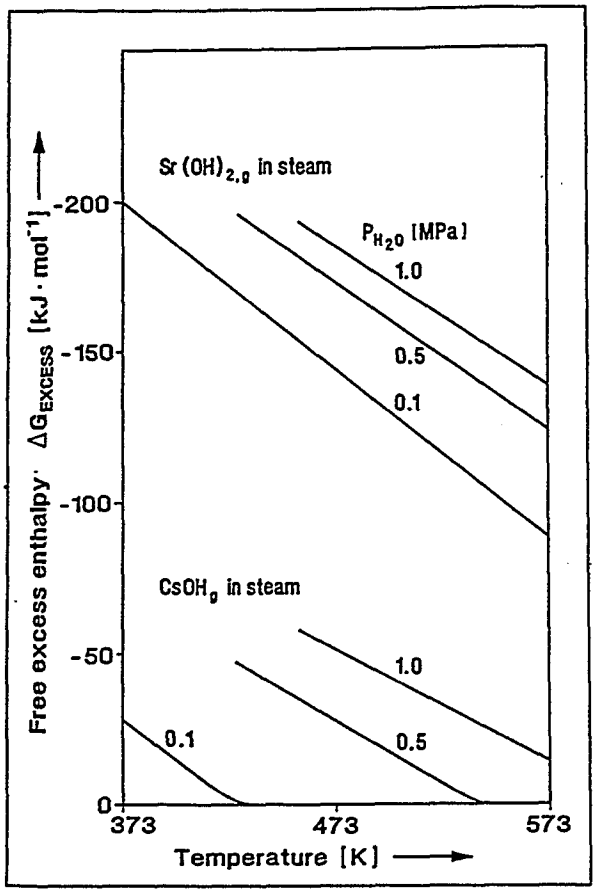

Free excess enthalpies of gaseous CsOH and $Sr(OH)_2$ in steam (estimated from experimental data of NaOH and BaO in steam)

Fig. B-1

Applying these data on HTR accident conditions one should bear in mind, that an extrapolation to steam partial pressures ≤ 1*MPa*, which are not covered by experimental data, is necessary. Fig. B-1 contains the free excess enthalpies for HTR-relevant steam partial pressures. Whereas the absolute amount of this free excess enthalpy does not increase above 60 $kJ \cdot mol^{-1}$ for CsOH, values of 200 $kJ \cdot mol^{-1}$ are possible in case of $Sr(OH)_2$.

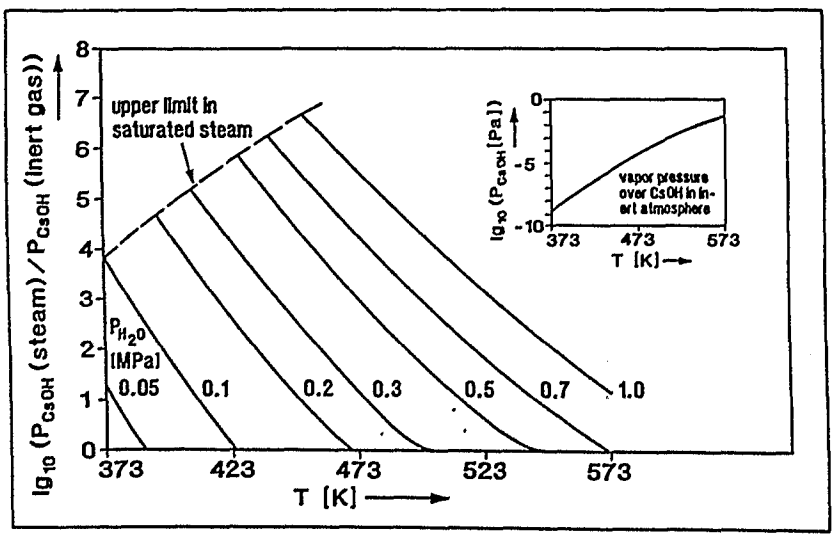

'Solubility' of CsOH in steam : Increase factors of CsOH-vapor pressure over pure CsOH depending on temperature for different steam partial pressures (estimated data on basis of NaOH behaviour in steam)

Fig. B-2

Fig. B-2 shows data of the vapor pressure increase over pure solid CsOH in presence of steam evaluated using eq. (B3). A significant vapor pressure increase of several orders of magnitude is possible also for water ingress accident conditions of

small HTR's at temperatures ≤ 573 *K*; the absolute vapor pressures in the steam influenced regime, however, do not exceed 10 *Pa*. Vapor pressures of $Sr(OH)_2$ are still more increased due to influence of steam; because of the low volatility of oxidic strontium compounds its absolute values remain however much less than those of CsOH in steam.

In general, this steam solubility effect has to be taken into consideration in wet atmospheres. Also, in presence of liquid water, eq. (B1) and (B2) should be used instead of partition coefficients between water and inert atmosphere.

The steam solubilty of fission product compounds could be important for LWR accident estimations too.

Appendix C: KINETICS OF AD/DESORPTION PROCESSES

With respect to plate out and desorption of fission products on metal or graphite surfaces the question arose, whether a spontaneous equilibrium on the surface may be assumed or not. Some models consider explicitely the ad/desorption kinetics on the surface, whereas the most applied models use sorption isotherms, i.e. sorption equilibrium.

Looking in detail, the overall plate out process consists mainly of two different processes, ad/desorption and mass transfer to/from the gas bulk. The time constanst of both processes should be evaluated. For the pure unactivated ad/desorption without hindrance by mass transfer holds:

$$d\sigma/dt = \vartheta \cdot \sigma - v \cdot c \qquad mol \cdot m^{-2} \cdot s^{-1} \qquad (C1)$$

with

v=average gas atom velocity=$(RT/2\pi M)^{0.5}$ $m \cdot s^{-1}$

ϑ=desorption constant=$10^{11} \cdot \exp(-\Delta H_{des}/RT)$ s^{-1}

M=mol mass $kg \cdot mol^{-1}$

c=fission product concentration in gas $mol \cdot m^{-3}$

σ=fission product concentration on the geometrical surface $mol \cdot m^{-2}$

The characteristic time constant is $\tau_{Ad}=\vartheta$. For mass transfer the characteristic time constant is

$$\tau_M = \beta \cdot c/\sigma \qquad s^{-1} \qquad (C2)$$

which leads for spontaneous ad/desorption equilibrium to:

$$\tau_M = \beta \cdot \vartheta/v \qquad s^{-1} \qquad (C3)$$

Comparison of both time constants results in:

$$\tau_{Ad}/\tau_M = v/\beta \qquad (C4)$$

Basic physics requires $v/\beta \geq 1$; for most relevant conditions, v is more than 3 orders of magnitude greater than β. Accordingly, the rate limiting step in the whole process is mass transfer and the assumption of a spontaneous ad/desorption equilibrium in combination with mass transfer is adequate for HTR safety calculations. An additional consideration of kinetics of the pure unactivated ad/desorption process as done in the

past in some models is superfluous. The latter is true not only for fission product plate out on metals but also on graphite.

An explicit consideration of the ad/desorption kinetics is reasonable only for the additional assumption of an activated ad- and desorption: In case, that the activation barrier of the ad/desorption process passes significantly over 30 $kJ \cdot mol^{-1}$, a basically mass transfer controlled handling would have to be replaced by sorption kinetic models; however, with respect to sorption of metallic fission products on metals there are only some indications for activation barriers in case of cesium on Inconel 617 /18,62/.

Appendix D: INFLUENCE OF TRAPPING DIFFUSION IN GRAPHITE ON SOURCE TERMS

Diffusion profiles of Cs in graphites indicate, that the diffusion mechanism cannot be explained by simple Fickian diffusion but requires a trapping diffusion model. This model does not only consider diffusion sites but also traps within the graphite. The trapping rate in graphite is given by /70,89/

$$\Phi_t = \mu \cdot c_D \quad mol \cdot m^{-3} \cdot s^{-1} \tag{D1}$$

with

μ = trapping coefficient s^{-1}
c_D = Cs-concentration on diffusion sites $mol \cdot m^{-3}$

and the emission rate from traps obeys

$$\Phi_e = b \cdot m \quad mol \cdot m^{-3} \cdot s^{-1} \tag{D2}$$

with

b = emission coefficient s^{-1}
m = Cs-concentration on traps $mol \cdot m^{-3}$

Values for μ and b and of their temperature dependence are experimentally determined for Cs at low concentrations in A3-3 material /70/.

The overall transport within the graphite is described by:

$$\delta c_D/\delta t = D \cdot (\delta^2 c_D/\delta x^2) - \mu \cdot c + b \cdot m \quad mol \cdot m^{-3} \cdot s^{-1} \tag{D3a}$$
$$\delta m/\delta t = \mu \cdot c_D - b \cdot m \quad " \tag{D3b}$$

with D = diffusion coefficient $m^2 \cdot s^{-1}$ (for data on A3-3 see /70/), which is correlated to the effective diffusion coefficient D_{eff} of the Fickian model by:

$$D_{eff} = D/(1+\mu/c) \quad m^2 \cdot s^{-1} \tag{D4}$$

Within this model, the sorption equilibria (represented by the Henrian coefficient α) of Cs on graphite are given by:

$$\alpha = c/(m+c_D) \tag{D5}$$

with

c = Cs-concentration in gas $mol \cdot m^{-3}$.

Calculations of sorption kinetics on graphite with the trapping diffusion model in comparison with the Fickian model indicate the following (initial Cs-burden in graphite=0):

Due to the activation effect in trapping, the overall sorbed amount of Cs in graphite is at beginning of sorption by a factor

$$f_r = (1+\mu/b)^{-0.5} \qquad (D6)$$

smaller in the trapping diffusion model than in the Fickian model. However, this difference decreases with increasing Cs-burden and vanishes for equilibrium conditions.

In order to find out the influence of the trapping effect on the overall Cs-source term in core heat-up events, FRESCO-calculations have been performed with and without the factor $1/f_r$ applied on the experimentally determined Henry coefficient α (evaluated from sorption isotherms). The results show, that the Cs-release out of the core cavern is by a factor of < 8 greater in core heat-up events of the HTR-Modul if trapping diffusion is taken into account; this factor represents an upper limit of the influence of the trapping diffusion for these particular accidents; the overall Cs-release out of the core cavern remains « 10^{-8} even with this factor and the increase by trapping diffusion remains insignificant from a radiological point of view.

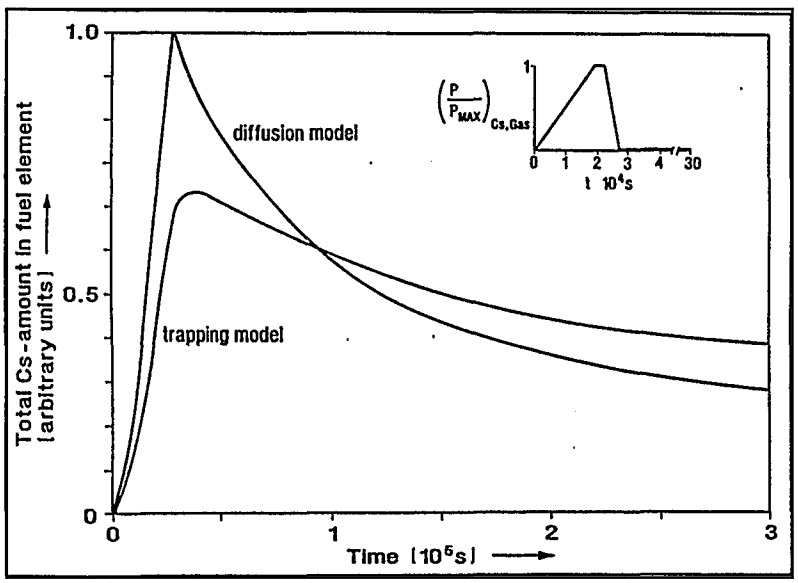

Total sorbed Cs-amount in an HTR fuel pebble for a given Cs partial pressure transient in the gas phase at 1000 °C = 1273 K • Comparison of Fickian diffusion and trapping model (Code FALLDIF)

Fig. D-1

It may therefore be concluded, that the usually applied Fickian diffusion model in graphite is a reasonable tool for safety estimations of small HTRs.

A code (FALLDIF) has been developed in KFA-ISR allowing for

solving the above given diffusion equations for cartesian and spherical geometries. As an example, fig. D-1 contains results of this code (concentration of Cs on diffusion sites and traps in a fuel element at 1000°C=1273 K) for a Cs concentration in the gas increasing linearly between 0 and 5 h to the maximum value, remaining for 1 h at this value and decreasing within 1 h to 0.

Appendix E: METHODS AND RESULTS OF DOSE ESTIMATIONS FOR SMALL SIZED HTRs

One reasonable tool for dose estimations in particular for small HTRs is defined in the German BMI calculation guidelines /4/, which were developed in principle only for LWR design basis accidents, but may be applied also for HTRs and other reactors and hypothetical events, provided, the corresponding source terms remain small. These guidelines are based with concern to atmospheric dispersion on a simple Gaussian model. Six Pasquill weather categories have to be considered together with wash-out and fall-out effects. Incorporation pathways modelled are inhalation and ingestion, external irradiation pathways are covered by cloudshine and groundshine. Resuspension is not part of the original BMI-guidelines but was taken into account in an extended KFA-model, developed for dose calculations of small HTRs. Generally spoken, these guidelines (including its data base) tend to give moderately overestimated maximum doses for a wide range of weather conditions, except probably for the ingestion pathway where conservatisms seem to be considerably larger (ingestion of the highest contaminated food of the whole area -except of the inner radius of 1 km around the emission point for accident times > 1 day after emission start- is assumed for the reference person). This BMI-dose estimation method has also been applied in FRG for calculations with respect to planning of catastrophic countermeasures /73/; in doing this, the BMI-dose estimation method has to be changed with respect to the particular requirements of catasprohic countermeasures, as indicated in table E-I:

Rule	Method of dose calculation	Dose limits [mSv] effective	thyroid	others
BMI calculation guidelines (§28.3 Str Sch V)	• ingestion (for distances <2000 m from emission point and times >24 h after accident initiation, directly contaminated plants are with drawn from food chains) inhalation, ground shine, submeirsion • no protective measures • 50 y exposure on worst location, incorporation of highest contaminated food • accumulation of internal irradiation over 50 y	50	150	300 (600 for skin)
ICRP-40 early phase, • sheltering • evacuation	•inhalation, ground shine •7 d exposure •accumulation of internal irradiation over 50 y	5-50 50-500	50-500 500-5000	
intermediate phase, • foodstuff control	• ingestion • 1 y exposure • accumulation of internal irradiation over 50 y	5-50	50-500	
• relocation	• ground shine, resuspension • 1 y exposure • accumulation of internal irradiation over 50 y	50-500	—	

Dose limits relevant for safety assessments of small sized HTR's

Table E-I

This table contains an overview on the BMI-guidelines and the corresponding dose criteria, valid for LWR design basis accidents together with the relevant

ICRP-40 doses and dose criteria for early and intermediate counter measures /71/. ICRP-40 is the basis for the corresponding German rules /5/.

Starting with the BMI- and ICRP-40-dose limits the single nuclide releases leading to these dose values have been estimated by application of the dose estimation methods of the BMI-guidelines, resp. by a slightly extended model, based on these guidelines; the particular needs of catastrophic planning (see table E-I) have been considered by this extended model.

Nuclide	Overall inventory in a 200 MW_{th} HTR-Modul [GBq]	BMI-calculation guidelines (§ 28.3 Str Sch V) effective emission height		ICRP-40 effective emission height					
		20 m	50 m	20 m sheltering	20 m relocation	20 m foodstuff control	50 m sheltering	50 m relocation	50 m foodstuff control
Kr-88	$2.22 \cdot 10^8$	$1.1 \cdot 10^6$	$2.1 \cdot 10^6$	$1.1 \cdot 10^5$	—	—	$2.1 \cdot 10^5$	—	—
Sr-90	$1.37 \cdot 10^7$	1.4	2.2	50	dose limits are exceeded only for source terms which require evacuation	0.9	100	dose limits are exceeded only for source terms which require evacuation	1.5
Ag-110m	$1.89 \cdot 10^5$	270	410	900	480	25	1800	730	48
I-131	$2.07 \cdot 10^8$	5.5	10	170	dose limits are exceeded only for source terms which require evacuation	0.25	350	dose limits are exceeded only for source terms which require evacuation	0.5
Xe-133	$4.44 \cdot 10^8$	$5.7 \cdot 10^7$	$1.1 \cdot 10^8$	$5.7 \cdot 10^6$	—	—	$1.1 \cdot 10^7$	—	—
Cs-134	$1.45 \cdot 10^7$	110	180	600	550	4.5	1100	830	8
Cs-137	$1.67 \cdot 10^7$	30	50	1300	1250	8.5	2500	1900	14

Remarks on ICRP-40:
- Evacuation thresholds are 1 order of magnitude higher than for sheltering (or more, if sheltering is explicitely considered before evacuation)
- Calculations are based on lower dose limits of ICRP-40
- Dispersion and exposure models used are those of BMI-calculation guidelines (§ 28.3 Str Sch V)
- No foodban was considered (in contrast to BMI-calculation guidelines for the inner radius) in threshold estimation for foodstuff control
- Thresholds are valid for the critical age (adult or infant) and for the critical organ

Source term thresholds [GBq] for single nuclides (short term emission) leading to a transgression of dose limits within a distance of ≥100 m from emission point

Table E-II

Table E-II shows maximum tolerable single nuclide releases of HTR key fission products, which do not lead to a transgression of the above mentioned dose criteria. The source terms are assumed to occur as a 1 *h* release, the plant boundary is 100 *m* from emission point. The table contains only results for effective stack heights of 20 and 50 *m*; one should bear in mind in this context, that an increase of stack heights decreases the maximum individual doses. The same is true, if the plant area (which has not to be considered in dose estimations) is assumed to be larger than a circle of 100 *m* around the emission point. It may be seen from table E-II, that BMI dose criteria for design basis accidents also cover ICRP-40 criteria except for noble gases (which are less

important from a radiological point of view, as the high tolerable source terms indicate) and for foodstuff control (which is a countermeasure that can be realized much easier and with a much better benefit to disadvantage relation than the others). Accordingly, if BMI-dose criteria are not reached, it may be concluded (at least for a first rough approximation), that emergency countermeasures except foodstuff control (in a small range around the plant) are not necessary. This conclusion is of particular importance, because BMI-dose criteria have sometimes solely been used for safety assessments of small HTRs including hypothetical events. Also, table E-II gives an idea what nuclear power nearly 'free off catastrophic events' means with respect to source terms.

Comparing the source terms presented in chap. 4 with the dose limits of tab. E-II it may be seen, that transgression of BMI-dose limits cannot be completely avoided for accidents of the HTR-Modul, which are however far beyond the scope of design basis events. Nevertheless, also for these cases the transgression remains below 1 order of magnitude. Catastrophic countermeasures (except perhaps milk control in the surrounding of the plant) are not necessary for the accident sequences examined in chap. 4, i.e. the frequency range of $\geq 10^{-7}\ a^{-1}$.

Appendix F: CRITICAL DISCUSSION OF PHYSICAL BACKGROUND AND DATA BASE OF THE PLATE-OUT MODEL PATRAS

A short description of the plate out model PATRAS and its data base for Cs is found in /75/. For this model it was claimed, that general physics and data base are as far as possible representative for HTR conditions; on the other hand, results generated with this code substantially differ from those of nearly all other models in the HTR field, in particular with respect to volume effects in the metal/oxide. Accordingly, a critical discussion of this model seems to be necessary and will be presented here. In comparing PATRAS code/data sets with others, it is important to note, that desorption constants of PATRAS are calculated with a preexponential factor of $1.3 \cdot 10^{11} \cdot T$, which is about 3 orders of magnitude higher than usually assumed (e.g. formula (1a) considers a desorption constant of 10^{11}, see eq. (C1)). Applying the PATRAS preexponential factor always leads to higher desorption enthalpies.

The basic parameter of this model ist the penetration coefficient π_p, representing the penetration (or absorption) probability of a nuclide, bouncing onto the metal surface. The model was primarily developed on the basis of experiments of fission product plate out on titanium (often used in AVR-VAMPYR-I, s. example of plate out curves in /60/). Most experiments on titanium can be sufficiently described by the penetration model. However, it was shown later by Wooley /77,79/, that titanium is a special case due to its fast growing oxide layer at $T > 873$ *K* (the titanium affinity to oxygen is very high). Similarly fast growing layers were not found in HTR metals. Therefore the main effect of penetration in titanium seems to be, that the growing oxide layer covers the adsorbed particles. One should bear in mind in this context, that the 'penetration effect' in titanium is due to an inclusion process and is, accordingly, dependent on oxygen potential and probably on temperature (influencing the oxide growing rate), which is not considered in PATRAS with its solely material and nuclide dependent penetration coefficient. Despite to its relative success in describing the plate out behaviour on titanium one should therefore note, that the penetration coefficient also for this case seems to be more or less an empirical parameter and the physical model behind it seems not to be sufficient.

The penetration model, developed for titanium, has been sometimes taken as applicable for HTR relevant materials too. Values of about 10^{-3} for

the penetration coefficient are given in /75/ for HTR materials; for silver a value of $2 \cdot 10^{-4}$ is proposed. Looking on these 'small' values one should bear in mind, that the penetration coefficient corresponds to the molecular velocity v (about 100 *m/s* for conditions relevant here, s. Appendix C) and not to the diffusion (mass transfer) velocity in the boundary layer ($0.005 \leq \beta \leq 0.2$ *m/s*). In detail, if $\pi_p \cdot v > \beta$, the plate out behaviour becomes mass transfer controlled in this model; this is already the case for cesium, if $\beta < 0.1$ *m/s*, which is true for most plate-out experiments. Following that, there should be a mass transfer controlled, temperature independent plate out profile in these experiments; this is not the case for their high temperature part (s. fig. F-1 for Cs on 15Mo3 in VAMPYR-I, PATRAS-calculations performed by INTERATOM /82/), indicating, that the penetration is much smaller than assumed by the PATRAS data base. (The mass transfer control in the low temperature part is due to adsorption, which is dominant under these conditions and allows the metal acting as a black body).

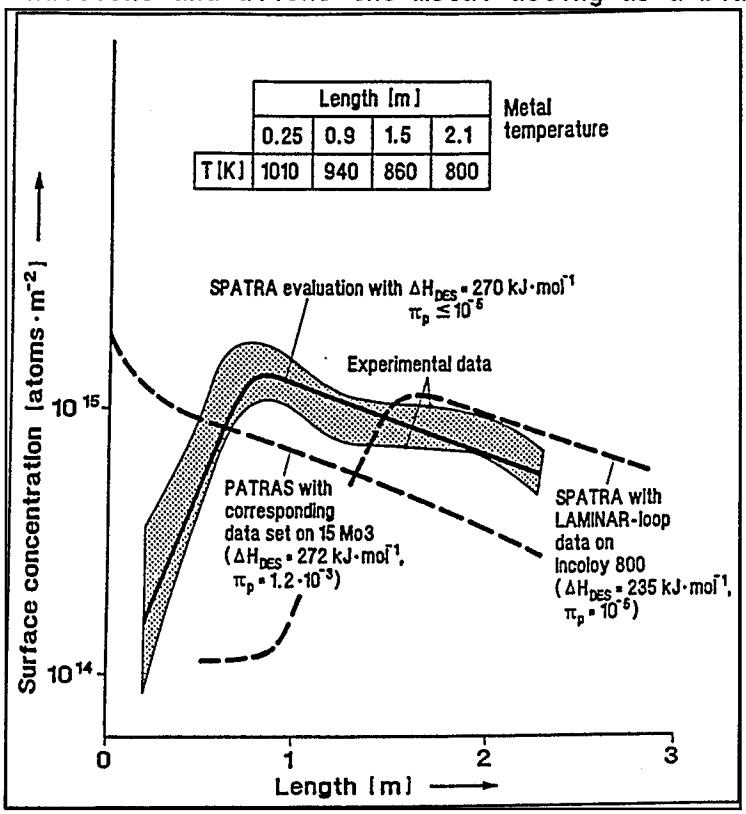

VAMPYR-I-09 · Cs-137 plate out evaluation on 15Mo3

Fig. F-1

A reasonable interpretation of the experiments is possible only by strong reduction of the penetration coefficient in relation to /75/, as the SPATRA calculation indicate (desorption enthalpy for 15Mo3: 270 $kJ \cdot mol^{-1}$, $\pi_p \leq 10^{-5}$). It seems to be a little bit difficult to understand, why the PATRAS results, presented in fig. F-1, are quoted in /48/ as to be in good agreement with the experiments. Similar results are obtained for VAMPYR-II (see fig. G-1 for cesium).

In case of Ag plate out in VAMPYR-II (s. fig. 6) PATRAS calculations (performed by INTERATOM /82/) again lead to a temperature independent plate out curve in strong contrast to the experimental behaviour; the

PATRAS reference value for π_p of silver however is smaller than for cesium, so that the plate out rate remains below the mass transfer limit; on the other hand, the desorption enthalpy is assumed here so small, that adsorption is always smaller than penetration.

There are no plate out experiments on HTR-materials, allowing for penetration coefficients of the above mentioned size: This also holds for experiments like SAPHIR-PEGASE P05, as explained in chap. 3.3, or the KFA-DRAGON hot gas experiment on Incoloy 800 ($700°C$ = $973\ K$), whose sucessfull interpretation with large penetration coefficients /96/ was due to a severe underestimation of the source concentration of cesium: With carefull reestimations of that source it was shown, that the penetration effect is much smaller /18,62/ and fits well the assumed range of $\pi_p=10^{-5}$. In addition, concepts of a hot gas filter taking credit of high penetration coefficients as given in /75/ were not sucessfull in AVR (see App. G), indicating, that such high penetration coefficients are not realistic. It is important to note in this context, that plate out in the Peach Bottom and AVR primary circuits can be sufficiently evaluated only without strong absorption /46/ resp. /95/ and fig. 7 in /48/. Plate out experiments in the LAMINAR-Loop /18,62/ can be interpreted by penetration coefficients, which are at least 2 orders of magnitude smaller than those of the PATRAS data set. Also, there are strong indications from Wooleys work, that not the penetration step itself is the rate limiting step but the diffusion process in the oxide layer, leading to a square root time behaviour of the absorption process (and of the penetration coefficient), which is not consistent with the assumptions of the PATRAS-penetration model. The decrease of absorptivity with time of Wooleys model may become, however, smaller, if inclusion acts as an additional absorption increasing effect.

Taking Wooleys data on absorption on oxidized reactor steel materials one can calculate a corresponding penetration coefficient (as a value averaged over time): The penetration coefficient averaged over a time period of 30 d is $1.5 \cdot 10^{-5}$, which is in good agreement with the LAMINAR-loop data for the same time period and also indicates, that the PATRAS data set heavily overestimates penetration effects. For longer time periods, the penetration coefficient evaluated from Wooleys data becomes still smaller than given above.

Furthermore, isotope effects in absorption, i.e. penetration coefficients different by a factor of two for Cs-137 and Cs-134, as have to be assumed in /75/, make no sense except perhaps for a long time scale,

when radioactive decay might affect penetrated activity more than adsorbed activity; but in that case penetration coefficients have to be assumed to be time dependent.

An important result of several postexaminations of plate out specimens is that significant amounts of metallic fission products can only be found in the oxide layer; a transport into the metal is possible only in case of a growing oxide layer: Cr-diffusion takes places during oxide growth, leading to a large number of vacancies, which support impurity transport from the oxide into the metal /76,78/. Also here the PATRAS data base is completely different: The oxide layer is considered to be the main penetration barrier with a very low diffusion coefficient, whereas diffusion in the metal proceeds much faster. PATRAS does not explicitely consider a thermochemical partition coefficient between oxide and metallic layer; deviations from a partition coefficient of 1 are however to be expected due to the completely different chemical environment for fission products in both phases. If the equilibrium concentration in the oxide phase is larger than in the metal phase, as many experiments indicate, the assumption of a very small diffusion coefficient in the oxide layer as in PATRAS is not adequate, because the barrier property of the oxide layer is caused by its stronger chemical interaction with the fission products in comparison with the metal layer.

In addition, from a physical point of view it is difficult to explain, that the absorption probability of a gas atom bouncing on a surface (= penetration coefficient of the PATRAS model) is independent on temperature (or kinetic energy of the gas atom) but depends for a given nuclide on some (temperature independent) material properties only: All processes leading to a transport into the volume (volume diffusion, grain boundary or micropore diffusion, or perhaps inclusion, which might similar as in titanium- contribute to the absorption) are coupled to a remarkable activation energy, which necessarily requires a temperature dependence of that penetration coefficient. However, if it is assumed that penetration does not occur directly from the gas phase but via the adsorbed state, this temperature independence (also found by Wooley for absorption rates at constant gas concentrations) becomes clear: The surface concentration decreases with increasing temperature due to increasing desorption, but the diffusion rate into the solid increases. Both effects may more or less compensate each other. The physical model of Herion /63/ (considering adsorption as a step between gas

and absorbed state) seems therefore to be more appropriate in describing volume effects than the PATRAS model, in particular, because the penetration model may cause misleading interpretations, if it is assumed as a 'physical' and not only as an empirical model. The Japanese plate out code PLAIN /92/ and also the main option of SPATRA take credit of the Herion description of volume effects.

Summing up, the data base given in /75/ for penetration coefficients seems not to be realistic but severely overestimates penetration effects. In addition, the physical model implemented in PATRAS is not very near to a correct description of the plate out process. Its remarkable success in a few postcalculations of plate out experiments is therefore probably due to a large number of free (fitting) parameters but not to a sufficient physical base. On the other hand, its a merit of the PATRAS model, that it first brought the attention on volume effects in plate out problems, which may be dominant in high temperature plate out (see. App. G), despite to the fact, that these volume effects are much smaller than assumed in /75/.

Knowing all the above mentioned restrictions, the penetration concept of PATRAS in combination with realistic penetration coefficients (data of LAMINAR-Loop /18/) may be taken as a rough method for estimation of volume effects during plate out, in particular of their influence on the shape of plate out profiles; this is especially true for low concentrations in the solid, where saturation effects ('solubilty'), which are not sufficiently known, play no role. The general applicability of a penetration model in the above given sense (i.e. a semiempirical model) is demonstrated by a number of the SPATRA calculations using the penetration option; part of these calculations are given in this chapter and in chap. 3.2 and app. G of this report.

Considering plate out models in general, one should bear in mind, that there are still some uncertainties (as described in chap. 3.3) which cannot be explained by existing models.

Appendix G: EXAMINATION OF VAMPYR-II PLATE OUT CURVES AND FILTER DEVICES

The VAMPYR-II plate out experiment of the AVR is described in /60/. It takes hot Helium gas of the AVR primary circuit and leads the gas through an Incoloy 800 tube (inner diameter 14 *mm*), containing an Inconel 617 slab of 9 *mm* diameter (length 3.6 *m*). It covers temperatures between 400°*C* = 673 *K* and 725°*C* = 998 *K* (in run 04 the temperatures were between 395°*C* = 668 *K* and 660°*C* = 933 *K*); experimental times and core exit temperatures are given in fig. G-3; the flow rate is 0.014 Nm^3/s at a total pressure of 1.08 *MPa*. Detailed results are documented in some internal reports /83/. In VAMPYR-II, a new kind of fission product filters, based on the penetration mechanism, were also tested behind the plate out section. Unfortunately, as shown below, these filters did not work properly in particular for Cs (although a sequence of 5 filters was used); the activity in an additional last (conventional, low temperature) filter was not measured and so a complete fission product balance cannot be made. A rough estimation of the total amount of fission products entering the test section in comparison with that, measured in VAMPYR-II, indicates, that the first is about a factor of ≤ 1.1 larger for Ag-110m than the later, but that this factor might be in the range of 1.5 (run 01) up to 5 (run 02) for Cs-nuclides; balance errors are smaller for Ag in all runs due to a strong Ag-sorption in the plate out section. However, comparing the integral measured Cs-amount of VAMPYR-II-01 with corresponding values calculated from VAMPYR-I-42 hot gas data, the first are by a factor of about 1.7 larger; also for Ag-110m VAMPYR-II-01 leads to larger hot gas concentrations than VAMPYR-I-42. This inconsistency (which is enlarged by the above given balance errors to a factor of about 2 to 2.5) might be taken as an indication of the size of the error with respect to the hot gas concentration of nuclides in the AVR. For VAMPYR-II-02 and -04 no parallel VAMPYR-I results are available.

Whereas silver plate out shows normal behaviour as explained by fig. 6, Cs plate out is unusual: The overall plate out is small and there is practically no temperature dependence of the plate out except for the very low temperature part (s. fig. G-1 for Incoloy 800 in run 01). In case of Inconel 617 /60/ the plate out curve remains completely flat, also in the low temperature range. One possible interpretation of this behaviour is the influence of dust on Cs plate out (although dust present in VAMPYR-I did not lead to remarkable deviations from normal

plate out behaviour on stainless steel): The amount of graphitic dust in the AVR primary circuit is comparatively high.

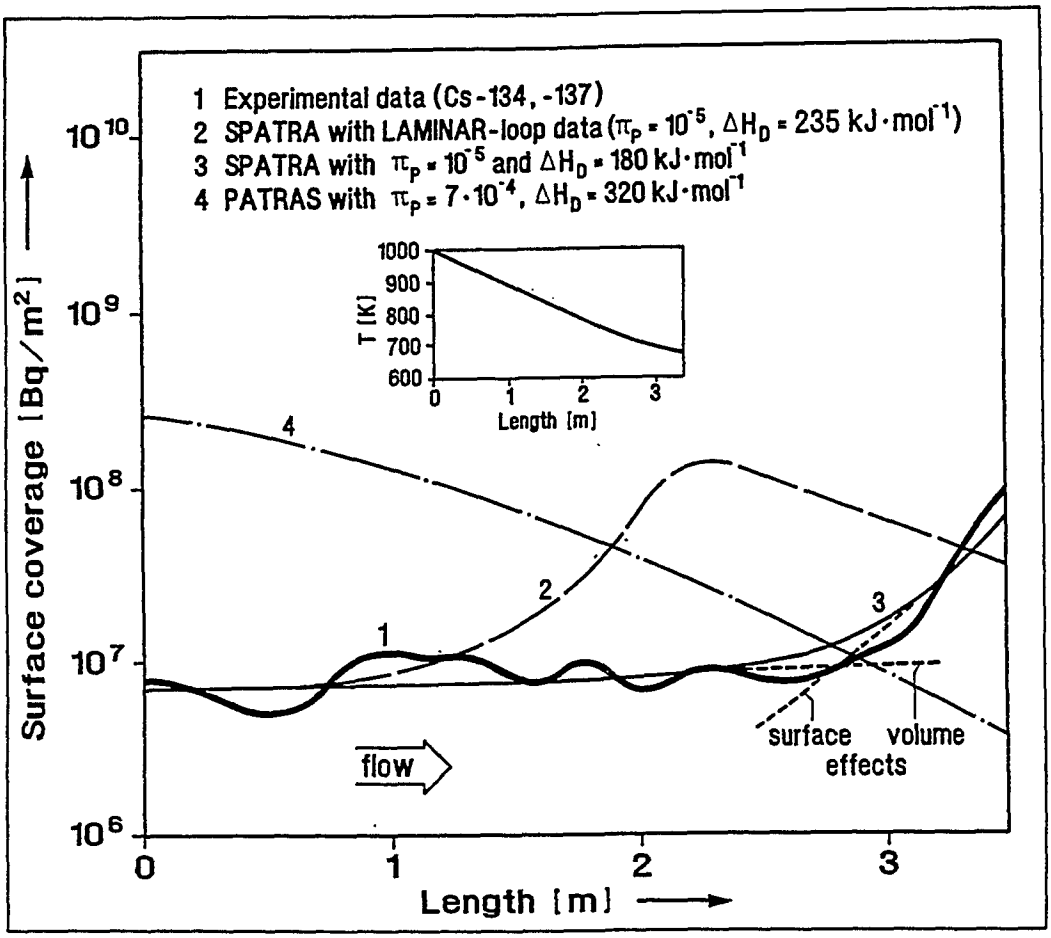

Cs-plate out on Incoloy 800 in VAMPYR-II-01 Comparison of experimental results with code calculations

Fig. G-1

In order to prove the assumption, that dust might lead to the unusual plate out behaviour, dust filter were installed in front and behind the plate out device /93/. The shape of the plate out profiles, however, remained unchanged, although the first filter retained more than 90 % of the gas borne dust found in this run 04, indicating, that dust is not the main reason for the unexpected cesium plate out. Fig. G-2 shows the distribution of 3 nuclides (Ag-110m representative for 'normal' plate out behaviour, Co-60 representative for dust borne nuclides and Cs-137): Whereas silver is mainly found in the plate out section and cobalt mainly in the first dust filter, cesium penetrates both equipments and is found in the second dust filter (behind the plate out section), which has a lower temperature than the first one. A similar behaviour has been observed several years ago in the COMEDIE-loop /80/, where 'normal' plate out was found for silver but small plate out with low temperature dependence for cesium on high temperature alloys; also

here, most of cesium was found in the filter behind the plate out section. Fig. G-3 shows the distribution of Cs-137 on the different parts of VAMPYR-II-01, -02, and -04.

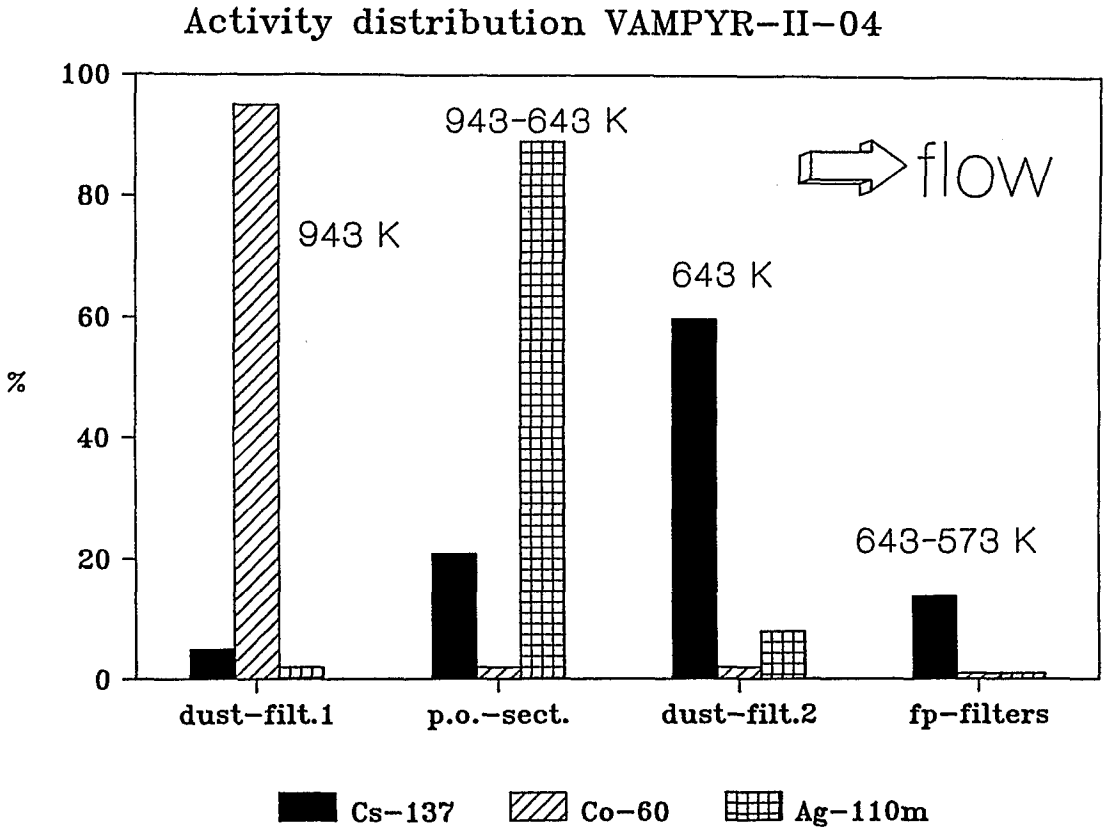

Fig. G-2

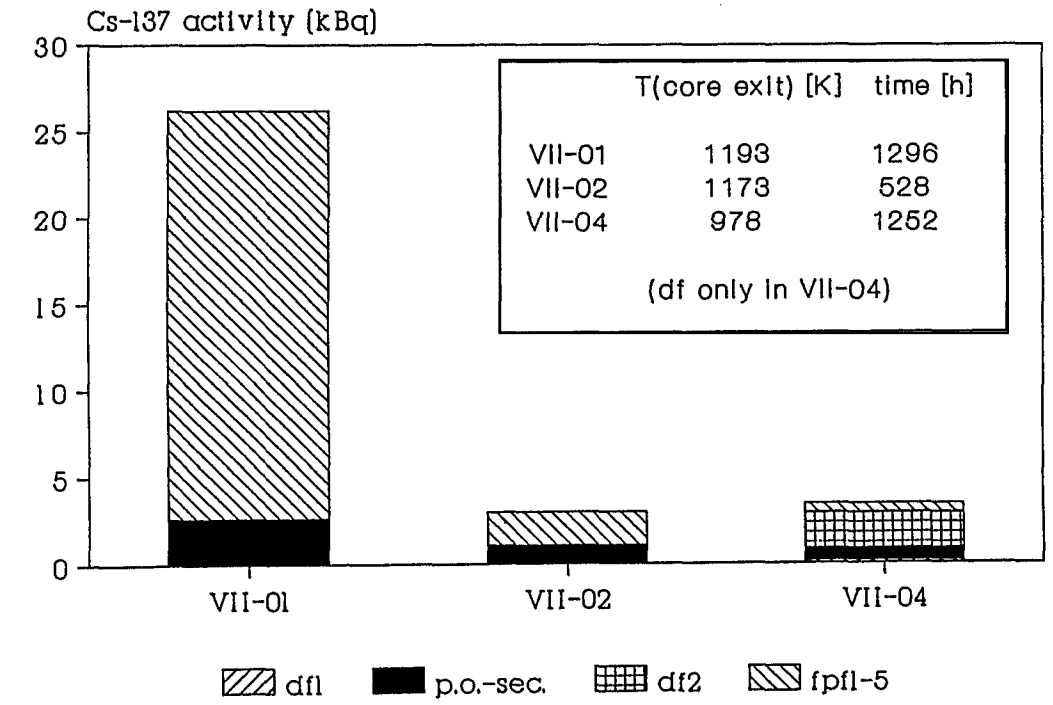

df=dust filter fpf=fiss. product filter

Fig. G-3

There is no reasonable interpretation for this behaviour of cesium in the moment on the basis of the plate out data published up to now: Fig. G-1 contains postcalculations of the plate out curves with the PATRAS model/data set (performed by INTERATOM /82/) and with SPATRA considering LAMINAR Loop data (the Cs-source was calculated from the integral Cs-amount found in VAMPYR-II, multiplied by a factor of 1.5 because of the insufficient working fission product filters). Whereas PATRAS, due to its high penetration assumption ($\pi_p=7\cdot10^{-4}$) leads to a very high plate out in the high temperature part, SPATRA with its 2 orders of magnitude smaller penetration coefficient ($1.0\cdot10^{-5}$) fits the plate out curve well in this range, but fails in the low temperature part. The high temperature range shows an approximately temperature independent sorption coefficient (defined in chap. 3.3 resp. /84/) of about 0.05, which indicates absorption/penetration, compatibel with the above SPATRA assumption. One should bear in mind, however, that in case, that the Cs-source is still larger than assumed here, a smaller penetration coefficient will be estimated, because the penetration coefficient shows an inverse proportionality to the source intensity for these conditions. A reasonable fit for the whole plate out profile is possible with SPATRA, if the desorption enthalpy of cesium is reduced by 55 *kJ/mol* to about 180 *kJ/mol* (π_p unchanged at $1.0\cdot10^{-5}$), as indicated in Fig. G-1; this decrease of desorption enthalpy shifts the strongly temperature dependent ad/desorption equilibrium range to lower temperatures. Similar interpretations of these plate out curves have been performed by HRB /81/ on the basis of their low temperature plate out experiments in the LAMINAR-Loop: At 440°*C* = 713 *K*, a lower desorption enthalpy than in high temperature experiments was observed; considering a temperature dependent desorption enthalpy, the cesium plate out in VAMPYR-II-01 can be explained fairly well; however, as the SPATRA calculation indicates, a reasonable fit can be obtained with only one (low) desorption enthalpy, too. One should bear in mind, that this successful postcalculation with SPATRA is not a sufficient argument for the general applicability of the simple penetration model for long term Cs plate out under normal operation conditions: As mentioned in App. F, a diffusion controlled absorption process might show pronounced differences in time behavior of absorption; these differences, however, could be diminished by inclusion, parallel to diffusion controlled absorption. Additional experiments with prolonged plate out period are therefore necessary in order to clarify this question (such experiments were

planned in VAMPYR-II, but could not be performed due to AVR final shut down.

Looking on the amount of cesium removable by water leach, this increases from about 25 % in the high temperature range to about 75 % in the low temperature range, as postexaminations revealed. Following the above given interpretation of the plate out curves, these values should be 0 % resp. ≤ 98 %: This is, because in the high temperature part only absorbed (penetrated) cesium occurs, for which no contact with liquid water has to be assumed; in the low temperature part adsorption dominates and water should wash off nearly all cesium it contacts due to the high solubility of all cesium compounds in water; however, it was already shown in chapter 3.3, that water does not reach all adsorbed cesium. The discrepancy here probably means, that there is no simple relation between wash off rate and ad- resp. absorption character of the plated out cesium, although the general tendency (increasing wash off fraction with decreasing temperatures) is the same for both, experiment and model calculation. PATRAS model/data, which strongly overestimate the penetrated fraction, accordingly underestimates the amount of cesium that can be washed off. This is only partly (in the low temperature range) compensated by the extraordinary high desorption enthalpies in PATRAS; nevertheless this means, that former analyses with PATRAS concerning cesium release in HTR water ingress events /39/ tend to underestimate corresponding source terms.

For Inconel 617 the desorption enthalpy of cesium has to be reduced to ≤ 165 *kJ/mol* in order to fit the VAMPYR-II-01 curve. Cs-balance errors seem to be larger in runs 02 and 04 in comparison with run 01: This can be deduced from the fact, that in runs 02 and 04 the relation of Cs in filters to the amount in the plate out section is significantly smaller than in run 01, although loading of the plate out section does not show anomalities (s. fig. G-3). If the same source rate as in run 01 is assumed for run 02 very similar results are obtained in evaluations with SPATRA; this assumption however means an increase of of the source rate in comparison with that calcualted from the integral Cs-amount in test sections and filters by about a factor of 5. For run 04 (which was performed at significantly smaller core temperatures, s. fig. G-3) a postcalculation similar to run 01 is possible, if the same relation of plated out to integral source activity as in run 01 is assumed, which leads to a source correction factor of about 3. There are only minor differences between between the shapes of run 01 and runs 02 and 04:

Examinations of the latter indicate, that the desorption enthalpy of cesium on Incoloy 800 might be still smaller than 180 *kJ/mol*. Also, the differences in surface coverage of slab and tube with Cs are slightly more pronounced in the high temperature part (with Inconel 617 slab having the smaller coverage) than for run 01. With respect to run 02 one should bear in mind, however, that besides the above mentioned large problems with the mass balance, there were a nitrogen ingress during operation and handling problems in postexamination of this run, which might enlarge the experimental error. Further experimental work is necessary in order to explain these experimental results respectively the low desorption enthalpy under these conditions.

With respect to the penetration problem (see App. F) one should bear in mind, that cesium plate out in VAMPYR-II can be explained only with penetration coefficients of $\leq 10^{-5}$, which is very low in comparison with /75/; however, due to the small desorption enthalpy, these penetration coefficients nevertheless influence significantly the plate out behaviour in the high temperature branch of VAMPYR-II.

Some information about silver plate out in VAMPYR-II in addition to that, already given in fig. 6 for Inconel 617 will be outlined here: The desorption enthalpy of silver on Incoloy 800 was estimated from run VAMPYR-II-01 to be about 255 *kJ/mol*, i.e. 15 *kJ/mol* higher than for Inconel 617. The other two VAMPYR-II runs which can be evaluated quantitatively with respect to Ag (02, 04) lead to similar desorption enthalpies for both metals. However, there are some differences in the penetration coefficient between the different experimental runs: For run 01 the penetration coefficient is in the range of $\leq 10^{-6}$ (and was consequently neglected in the SPATRA evaluations presented in fig. 6), whereas runs 02 and 04 indicate slightly higher penetration coefficients, which, however still remain $\leq 10^{-5}$.

The general interpretation of VAMPYR-II with respect to penetration/-absorption given here finds also support in evaluation of the fission product filters of VAMPYR-II: Behind the plate out section there are 5 fission product filters consisting on stainless steel 4541 and operating at temperatures of 300 - 400°*C* ≈ 573 - 673 *K*; the fission product filters were designed on the basis of the penetration model /94/, taking credit of high penetration coefficients; i.e. significant plate out by penetration was assumed to be the general working mechanism. A clear indication of sufficient working efficiency of that filters is a strong decrease of their fission product burden in direction of flow. This was

not observed for cesium in runs 01 and 02 (instead, an increasing Cs-burden was found in direction of flow, see fig. G-4); as mentioned above, the amount of Cs entering the filter device and not retained there might be very large.

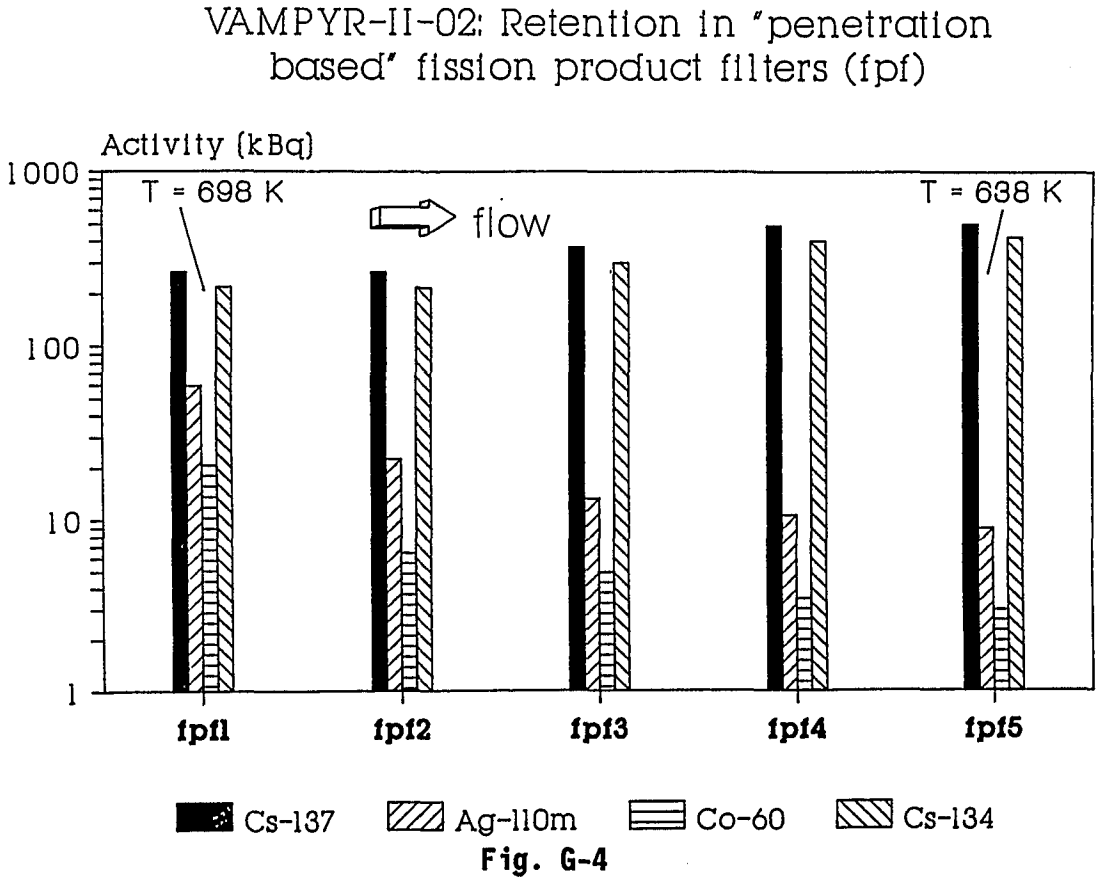

Fig. G-4

For Ag, a better retention was observed in all runs, which was, however, about 30 % per single filter (average value) and therefore still far from being sufficient. Co-60, which is clearly dust borne, shows a decreasing concentration in direction of flow in these filters; this means, that dust depletion behaves different from Cs-plate out and may be taken as an additional indication, that Cs is mainly not dust borne. Run 02 contained an empty dust filter box in front of the plate out section; a remarkable Co-60 (dust) depletion was found in this box. In run 04 a slightly decreasing Cs-concentration in flow direction was observed for the first 4 filters, followed by a significant reincrease in the last filter; this behaviour was also found for Co-60 and Ag-110m. The conditions in run 04 are not typical due to the fact, that the gas-concentrations of Cs in the fission product filter section are smaller than in the other runs; this is partly due to the lower core temperature and partly due to a dust filter: Interestingly, the single dust filter between plate out section and fission product filter device in run 04 had at least about the same filter efficiency for Cs than the 5

fission product filters in total (see. fig. G-2), although Cs is -as mentioned above- obviously not dust borne. Alltogether, the (penetration based) fission product filter efficiency was at least much smaller than expected on the basis of data in /75/, but in some cases nearly non existent; run 04 also indicates, that in searching of a fission product filter operating at temperatures > 300°C ≈ 573 K (in particular for mainly non dust borne Cs) it seems to be more effective to rely on the well known dust filter equipments than on special penetration based devices.

With respect to the Code SPATRA, the evaluations of the VAMPYR-II experiment together with those of VAMPYR-I may be taken as a partial validation.

FORSCHUNGSZENTRUM JÜLICH GmbH

KFA

Jül-2669
August 1992
ISSN 0366-0885